Supplementary Information

Conformation and orientation of branched acyl chains responsible for the physical stability of diphytanoylphosphatidylcholine

Hiroshi Tsuchikawa,[†,∥] Takuya Ono,[†] Masaki Yamagami,[†,‡] Yuichi Umegawa,[†,‡], Wataru Shinoda,[§,*] and Michio Murata[†, ‡,*]

[†] Department of Chemistry, Graduate School of Science, Osaka University, 1-1 Machikaneyama, Toyonaka, Osaka 560-0043, Japan

[∥] Department of Clinical Pharmacology and Therapeutics, Faculty of Medicine, Oita University, 1-1 Idaigaoka, Hasama-machi, Yufu, Oita 879-5593, Japan

[‡] JST ERATO, Lipid Active Structure Project and Project Research Center for Fundamental Science, Osaka University, 1-1 Machikaneyama, Toyonaka, Osaka 560-0043, Japan

[§] Department of Materials Chemistry, Graduate School of Engineering, Nagoya University, Nagoya 464-8603, Japan

Table of Contents

I. General information

Unless otherwise indicated, all reactions were carried out with magnetic stirring in oven-dried glassware under argon atmosphere. Commercially available reagents were purchased from Nacalai Tesque, Sigma-Aldrich, TCI, and were used without further purification. The dehydrated solvents dichloromethane (CH_2Cl_2) and tetrahydrofuran (THF) were purchased from Kanto Chemical Co. Inc. and were used without further dehydration. Analytical thin-layer chromatography (TLC) were carried out on Merck pre-coated silica gel 60 F-254 plates and revealed with UV irradiation (254 nm) and stained with phosphomolybdic acid. Flash chromatographies were performed with Biotage prepacked columns using a Biotage Isolera One purification system. ^{1}H and ^{13}C NMR spectra were recorded on a JEOL ECS 400 (400 MHz) or JEOL ECA 500 (500 MHz) spectrometer. Chemical shifts (δ) are given in parts per million (ppm) relative to the solvent residual peak of $CDCl_3$ (7.26 ppm for ^{1}H, 77.0 ppm for ^{13}C) or CD_3OD (4.78 ppm for ^{1}H, 49.0 ppm for ^{13}C). Splitting patterns are indicated as followed: s, singlet; d, doublet; t, triplet; q, quartet; oct, octet; m, multiplet; b, broad and combinations thereof. Coupling constants (J) are reported in hertz (Hz).

II. Synthesis of epDPhPC and ^{2}H-labeled epDPhPC

1) Retrosynthesis

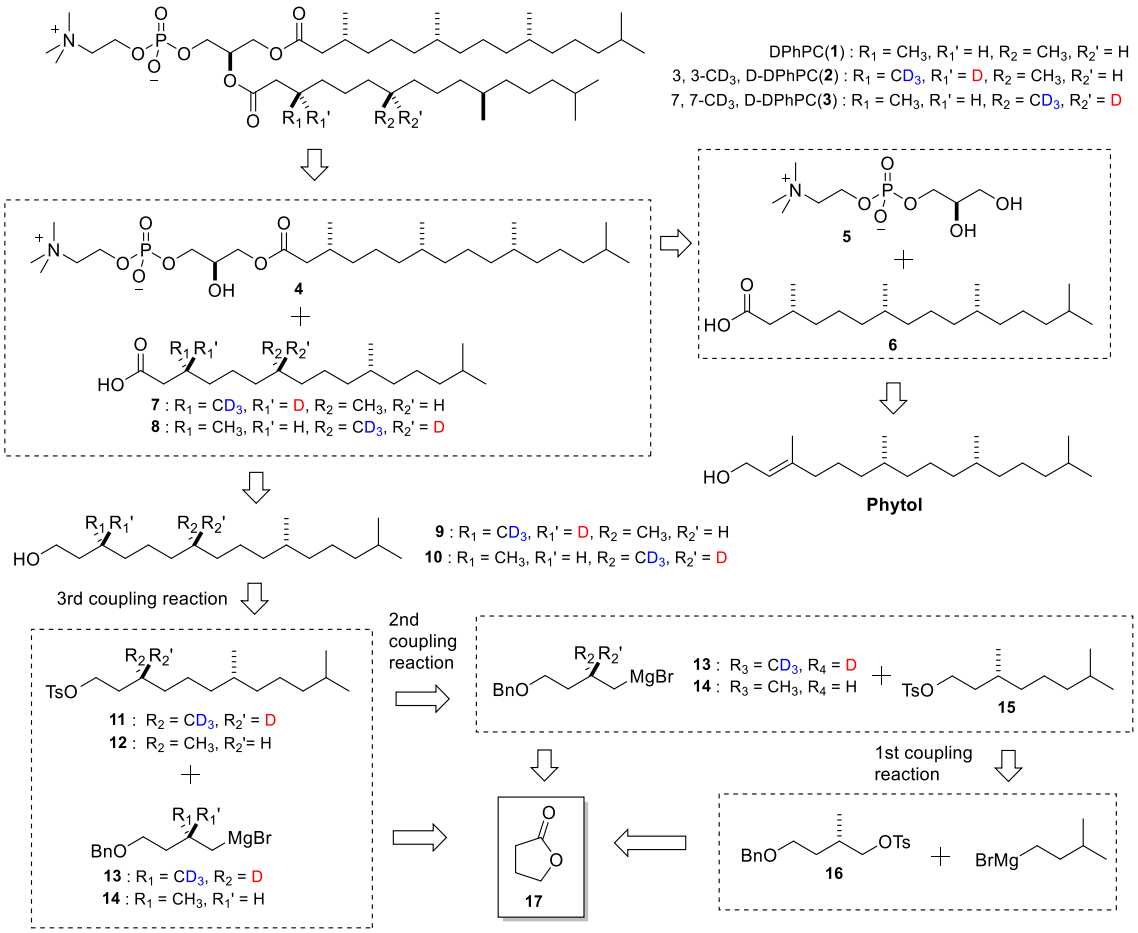

Scheme S1. Retrosynthetic route for epDPHPC **1** and deuterated epDPhPCs **2** and **3**

*2) Synthesis of ^{2}H-labeled isoprene units with high optical purity (**13**, **14**) and deuterium labeled phytanols (**9**, **10**).*

Deuterated phytanols (**9**, **10**) was synthesized by the previous method (ref. 22 of the manuscript) (Scheme S1). They were prepared in the common synthetic route only by changing the order of connecting isoprene units. That is, in the case of 3-position deuterium-labeled phytanol (**9**), deuterium-labeled Grignard reagent **13** was used in the 3rd coupling reaction with non-deuterated tosylate **12**, and in the case of 7-position deuterium-labeled phytanol (**10**), the deuterium-labeled Grignard reagent **13** was used in the 2nd coupling reaction. All isoprene units (**13, 14, 16**) with high optical purity were successfully synthesized from lactone **17** by following our established method (ref. 22).

3) Synthesis of deuterium labeled phytanic acids (7, 8)

The target deuterium labeled phytanic acids (**7, 8**) was synthesized by oxidizing the phytanyl alcohols (**9**, **10**) with Jones reagent (Scheme S2).

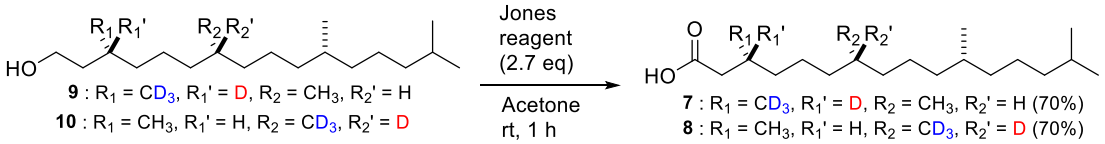

Scheme S2

C*D*$_3$,*D*-phytanic acids 7 and 8: To a solution of C*D*$_3$,*D*-phytanol **9** or **10** (110 mg, 0.36 mmol) in acetone (7.8 mL) was added Jones reagent (0.39 ml, 0.98 mmol) and the reaction mixture was stirred for 1 h at room temperature. Then quenched with water and the mixture was extracted with AcOEt (×3). The combined organic layer was washed with brine and dried over anhydrous Na_2SO_4, then filtered. Filtrate was concentrated, and the residue was purified with flush column chromatography on silica gel (EtOAc/Hexane = 2/5) to afford alcohol **7** or **8** (80 mg, 0.25 mmol, 70%) as a colorless oil.

7: colorless oil, Rf = 0.18 (hexane/ethyl acetate = 15/1); ^{1}H NMR (500 MHz, $CDCl_3$) 3.72-3.63 (m, 2H), 1.63-1.49 (m, 3H), 1.38-1.05 (m, 21H), 0.89 (d, *J* = 6.5 Hz, 3H), 0.90-0.83 (m, 12H); ^{13}C NMR (125 MHz, $CDCl_3$)

4) Synthesis of Lyso PC (4)

Lyso PC (**4**) was synthesized as shown in Scheme S3. First, unlabeled phytanic acid **6** was prepared from commercially available enantiopure phytol by asymmetric hydrogenation with a chiral ruthenium catalyst and the subsequent oxidization. After L-α-Glycerylphosphorylcholine (GPC) was converted to cyclic tin ester by treatment with *n*-dibutyltin oxide, *sn*-1 selective acylation was performed by adding a separately prepared phytanic acid chloride from the synthesized phytanic acid **6** to give the desired lyso PC (**4**) in 38% yield. The *sn*-1 selectivity was confirmed by ^{1}H NMR spectrum of the glycerol moiety of *lyso*-PC.

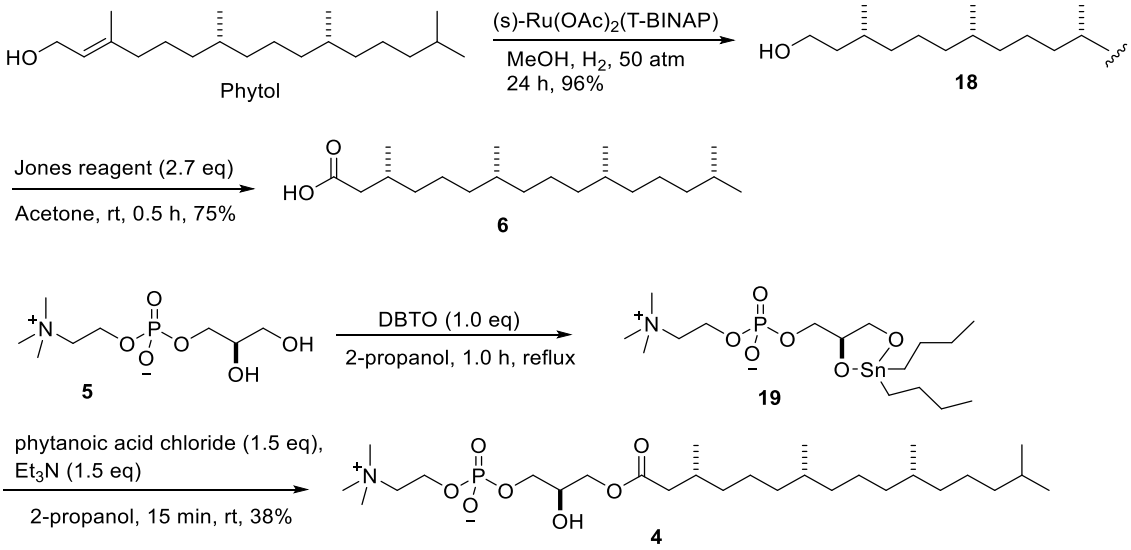

Scheme S3

Phytanol 18: To a solution of phytol (1.0 g, 3.4 mmol) in MeOH (15 mL) was added (s)-Ru(OAc)$_2$(T-BINAP) (61 mg, 0.067 mmol). The mixture was hydrogenated for 24 h under 50 atm of hydrogen gas. After concentration, the residue was purified by flush column chromatography on silica gel (gradient EtOAc/Hexane = 1/10 to 1/5) to afford phytanol **18** (0.97 g, 3.25 mmol, 96%) as a pale-yellow oil.

Phytanic acid 6: To a solution of Phytanol **18** (500 mg, 1.67 mmol) in acetone (45 mL) was added Jones reagent (1.81 ml, 4.52 mmol) and the reaction mixture was stirred for 1 h at room temperature. Then quenched with water and the mixture was extracted with AcOEt (×3). The combined organic layer was washed with brine and dried over anhydrous Na_2SO_4, then filtered. Filtrate was concentrated, and the residue was purified with flush column chromatography on silica gel (EtOAc/Hexane = 2/5) to afford acid **6** (390 mg, 1.25 mmol, 75%) as a pale-yellow oil.

Lyso-PC 4: Phytanic acid **6** (100 mg, 0.32 mmol) was added to the two-necked flask, and toluene azeotropy was performed three times and dissolved in toluene (2 ml). Oxalyl dichloride (41.2 µl, 0.48 mmol) was added and the mixture was stirred for 30 minutes, and then azeotrope with toluene twice to give phytanic acid chloride. GPC **5** (54.8 mg, 0.21 mmol) was added to the two-necked flask, dissolved in 2-propanol, DBTO (53.1 mg, 0.21 mmol) was added, and the mixture was heated under reflux for 1 hour. After cooling to room temperature, triethylamine (44.6 µl, 0.32 mmol) and prepared phytanic acid chloride were added and stirred for 15 min. The reaction mixture was extracted with water, washed with hexane three times, and the solvent was evaporated under reduced pressure. The residue was purified with flush column chromatography on silica gel ($CHCl_3$/MeOH/water = 65/25/0 to 65/25/4) to afford lyso-PC **4** (45 mg, 0.08 mmol, 38%) as a white solid.

4: white powder; R_f 0.40 ($CHCl_3$/MeOH/water = 65/ 35/4); ^{1}H NMR (400 MHz, $CDCl_3$/d_4-MeOH =

1/2) δ 3.88-3.82 (br, 2H), 3.76-3.63 (m, 2H), 3.56-3.40 (m, 3H), 3.22-3.16 (m, 2H), 2.78 (s, 9H), 1.94-1.63 (m, 2H), 1.53-1.43 (m, 1H), 1.12-1.02 (m,1H), 1.01-0.55 (m, 20H), 0.50 (d, J = 6.4 Hz, 3H), 0.44-0.38 (m, 12H); ^{13}C NMR (100 MHz, $CDCl_3$/*d*4-MeOH = 1/2) δ 177.7, 72.6, 72.6, 70.7, 70.7, 70.2, 70.2, 68.9, 63.1, 63.1, 57.6, 45.4, 43.2, 41.2, 41.2, 41.2, 41.1, 41.1, 41.1, 36.6, 34.2, 31.8, 28.6, 28.2, 28.2, 26.1, 26.0, 23.2, 23.2, 23.1

*5) Synthesis of epDPhPC (**1**) and deuterium labeled DPhPC (**2, 3**)*

Finally, the condensation of lyso-PC (**4**) with phytanic acids (**6, 7, 8**) was conducted using DCC and DMAP to successfully afford the objective epDPhPC (**1**) and 3,3-CD_3,D-DPhPC (**2**) and 7,7-CD_3,D-DPhPC (**3**) in 38%, 70% and 40% yields, respectively.

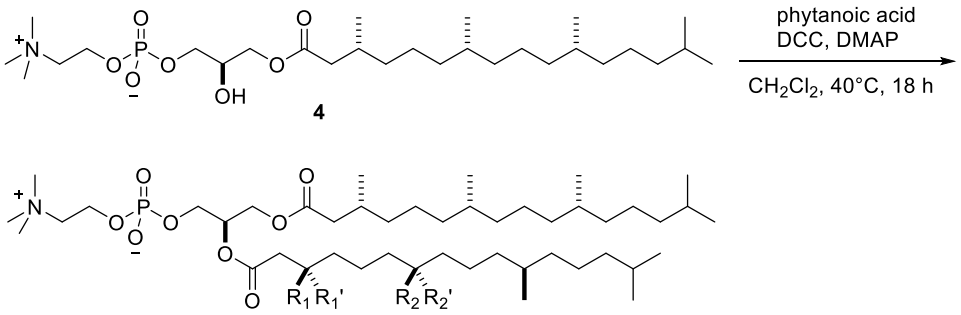

DPhPC(**1**) : R_1 = CH_3, R_1' = H, R_2 = CH_3, R_2' = H (38%)
3, 3-CD_3, D-DPhPC(**2**) : R_1 = CD_3, R_1' = D, R_2 = CH_3, R_2' = H (70%)
7, 7-CD_3, D-DPhPC(**3**) : R_1 = CH_3, R_1' = H, R_2 = CD_3, R_2' = D (40%)

Scheme S4

DPhPC (**1**): Phytanic acid **6** (92.1 mg, 0.29 mmol) and lyso-PC **4** (65.0 mg, 0.12 mmol) were added to flask and dissolved in dichloromethane (2.5 ml). DCC (102.2 mg, 0.49 mmol) and one piece of DMAP were added and refluxed for 18 h. The solvent was removed under reduced pressure, and the residue was purified by silica gel column chromatography (silica gel, $CHCl_3$/MeOH/water = 1/0/0 to 65/25/0 to 65/25/4) to afford DPhPC (**1**) (38.5 mg, 0.046 mmol, 38%) as a white solid.

1: white powder; R_f 0.80 ($CHCl_3$/MeOH/water = 65/35/4); ^{1}H NMR (400 MHz, $CDCl_3$/d_4-MeOH = 1/2) δ 4.84-4.77 (m, 1H), 4.00 (dd, J = 3.2, 12.0 Hz, 1H), 3.86-3.78 (m, 2H), 3.72 (dd, J = 7.6, 12.4 Hz, 1H), 3.57 (t, J = 12.4 Hz, 2H), 3,19-3.16 (m, 2H), 2.78 (s, 9H), 1.95-1.62 (m, 4H), 1.62-1.41 (br, 2H), 1.02-1.20 (m, 2H), 1.00-0.55 (m, 40H), 0.52-0.48 (m, 6H), 0.44-0.39 (m, 24H) ; ^{13}C NMR (100 MHz, $CDCl_3$/*d*4-MeOH = 1/2) δ 177.2, 176.8, 74.4, 74.3, 70.2, 67.5, 66.5, 63.1, 63.0, 57.6, 45.5, 45.4, 43.2, 41.3, 41.2, 41.2, 41.1, 41.1, 41.0, 40.9, 36.6, 34.3, 31.8, 28.6, 28.3, 26.1, 26.1, 23.3, 23.3, 23.1

3,3-C*D*$_3$,*D*-DPhPC (**2**): 3-C*D*$_3$,*D*-phytanic acid **7** (35.9 mg, 0.11 mmol) and lyso-PC **4** (25.0 mg, 0.045 mmol) were added to flask and dissolved in dichloromethane (0.8 ml). DCC (39.2 mg, 0.19 mmol) and

one piece of DMAP were added, and refluxed for 18 h. The solvent was removed under reduced pressure, and the residue was purified by silica gel column chromatography (silica gel, $CHCl_3$/MeOH/water = 1/0/0 to 65/25/0 to 65/25/4) to afford 3,3-C*D*$_3$,*D*-DPhPC (**2**) (27 mg, 0.032 mmol, 70%) as a white solid.

2; white powder; R_f 0.80 ($CHCl_3$/MeOH/water = 65/35/4); ^{1}H NMR (400 MHz, $CDCl_3$/d_4-MeOH = 1/2) δ 4.84-4.77 (m, 1H), 4.00 (dd, *J* = 3.2, 12.0 Hz, 1H), 3.86-3.78 (m, 2H), 3.72 (dd, *J* = 7.6, 12.4 Hz, 1H), 3.57 (t, *J* = 12.4 Hz, 2H), 3,19-3.16 (m, 2H), 2.78 (s, 9H), 1.95-1.62 (m, 4H), 1.62-1.41 (br, 1H), 1.02-1.20 (m, 2H), 1.00-0.55 (m, 40H), 0.52-0.48 (m, 3H), 0.44-0.39 (m, 24H)

7,7-C*D*$_3$,*D*-DPhPC (**3**): 7-C*D*$_3$,*D*-phytanic acid **8** (35.9 mg, 0.11 mmol) and lyso-PC **4** (25.0 mg, 0.045 mmol) were added to flask and dissolved in dichloromethane (0.8 ml). DCC (39.2 mg, 0.19 mmol) and one piece of DMAP were added, and refluxed for 18 h. The solvent was removed under reduced pressure, and the residue was purified by silica gel column chromatography (silica gel, $CHCl_3$/MeOH/water = 1/0/0 to 65/25/0 to 65/25/4) to afford 7,7-C*D*$_3$,*D*-DPhPC (**3**) (15 mg, 0.018 mmol, 40%) as a white solid.

3; white powder; R_f 0.80 ($CHCl_3$/MeOH/water = 65/35/4); ^{1}H NMR (400 MHz, $CDCl_3$/d_4-MeOH = 1/2) δ 4.84-4.77 (m, 1H), 4.00 (dd, *J* = 3.2, 12.0 Hz, 1H), 3.86-3.78 (m, 2H), 3.72 (dd, *J* = 7.6, 12.4 Hz, 1H), 3.57 (t, *J* = 12.4 Hz, 2H), 3,19-3.16 (m, 2H), 2.78 (s, 9H), 1.95-1.62 (m, 4H), 1.62-1.41 (br, 2H), 1.02-1.20 (m, 2H), 1.00-0.55 (m, 39H), 0.52-0.48 (m, 6H), 0.44-0.39 (m, 21H)

III. Evaluation of stereochemical homogeneity of comDPhPC and epDPhPC

1) Examination of stereochemical homogeneity of comDPhPC by using the 2-methoxy-2-naphtyl-propionate derivative of phytanol derived from its phytanoyl chains

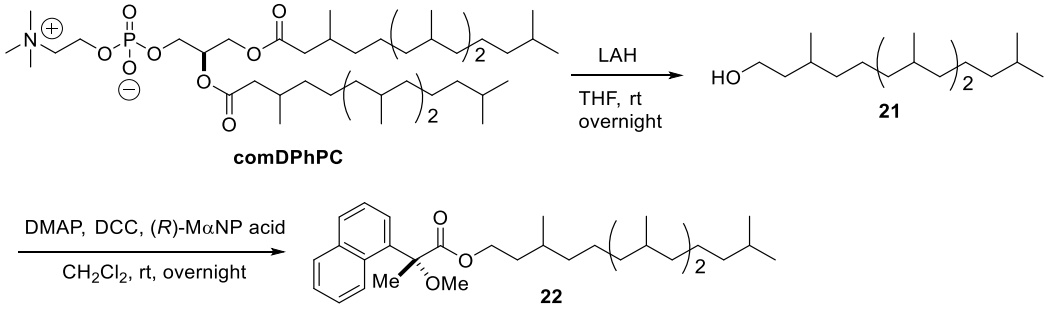

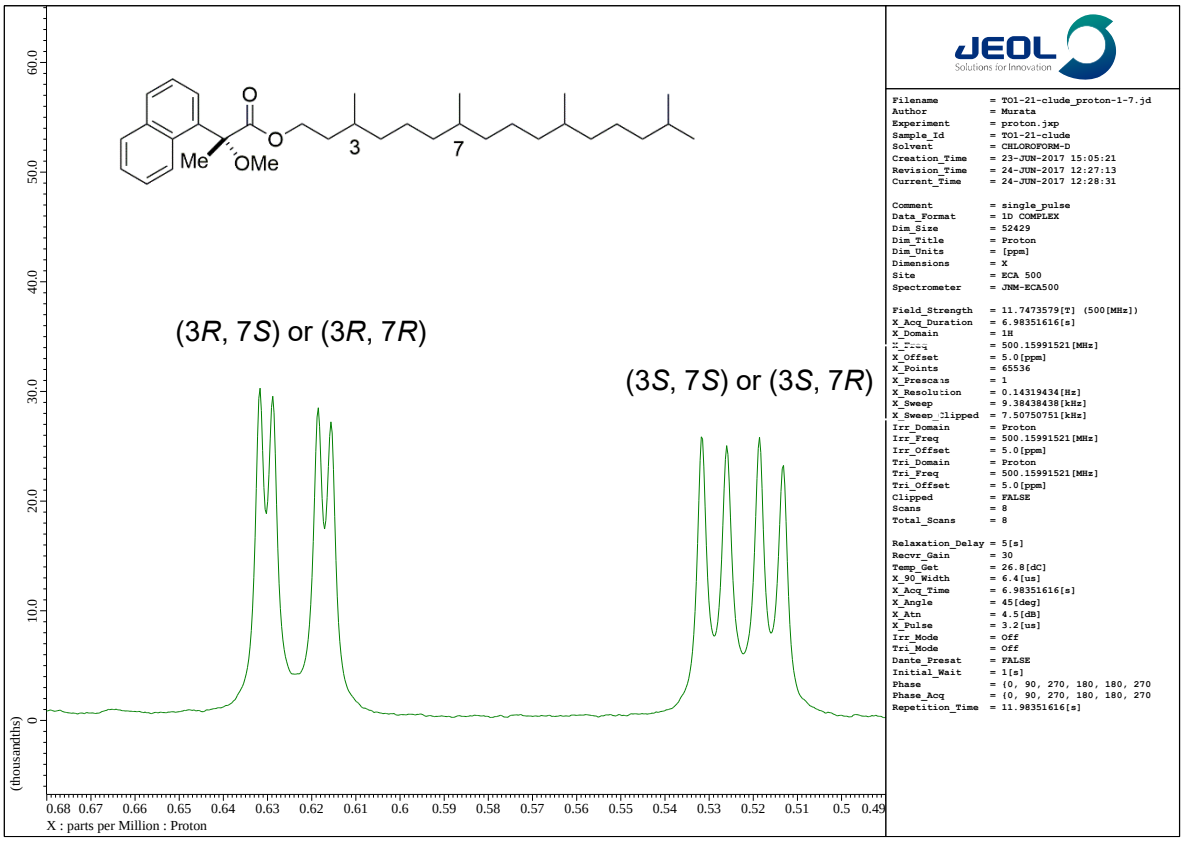

Figure S1. ^{1}H NMR spectrum of the (*R*)-2-methoxy-2-naphtyl-propionate derivative of phytanol derived from commercial DPhPC (comDPhPC) in $CDCl_3$ at 500MHz. Regarding the stereochemistry at the C3 or C7 positions of the phytanol derived from comDPhPC, the spectrum shows a nearly 1:1 diastereomeric mixture, respectively.

2) Examination of stereochemical homogeneity of epDPhPC by using the 2-methoxy-2-naphtyl-propionate derivative of phytanol derived from synthesized phytanic acid ***6***

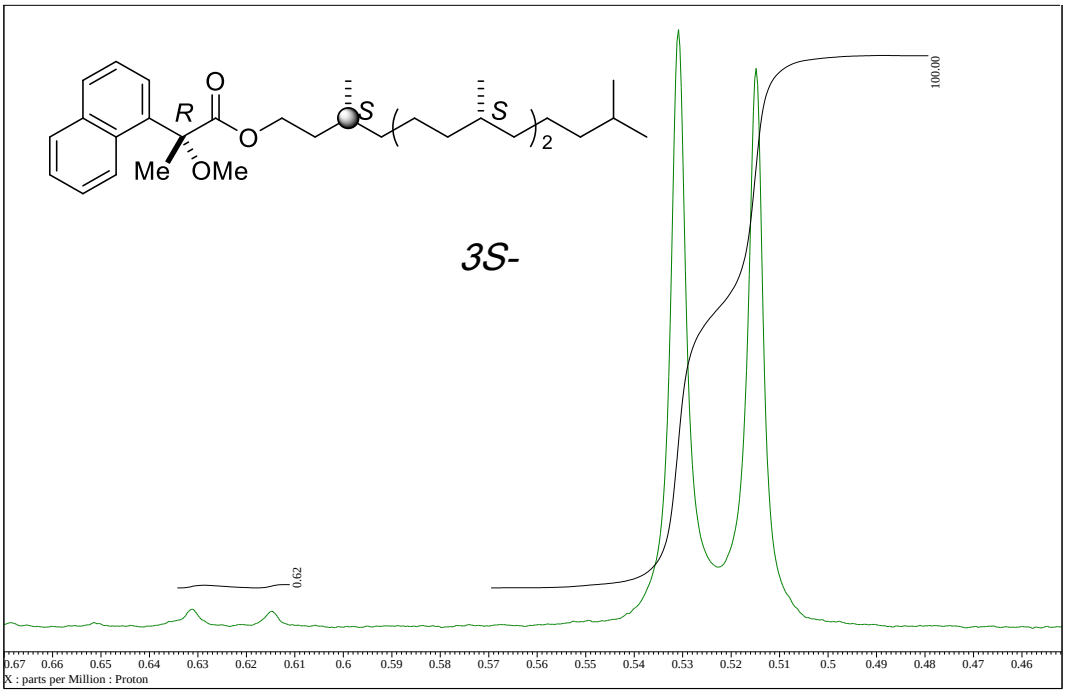

Figure S2. ^{1}H NMR spectrum of the (*R*)-2-methoxy-2-naphtyl-propionate derivative of phytanol derived from synthetic phytanic acid **6** ($CDCl_3$, 500MHz). Regarding stereochemistry at the C3 positions of **6**, the spectrum shows that the enantiomeric excess of **6** is higher than 99%.

IV. Measurement of water permeability

Water permeability parameter (P_f) was calculated by fitting the measured data (Fig S3) with the following differential equation.

$$dV_{(t)}/dt = (P_f)(SAV)(MVW)\left\{\left[C_{in}/V_{(t)}\right] - C_{out}\right\}$$

P_f is a water permeability parameter, *SAV* is the surface area relative to the volume of the liposome, *MVW* is the volume of water per mole, C_{in} is the solution concentration inside the liposome, and C_{out} is the solution concentration outside the liposome.

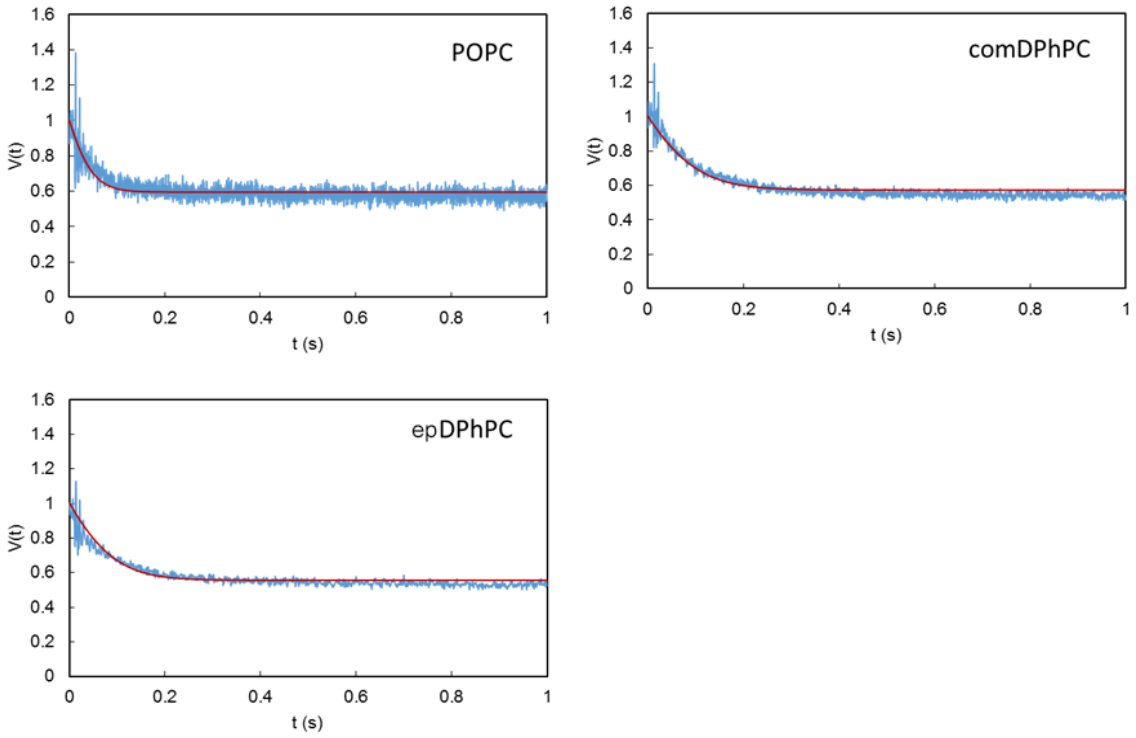

Figure S3. Measurements of water permeability of comDPhPC, epDPhPC and POPC LUVs

V. ^{2}H NMR measurements and orientation analysis

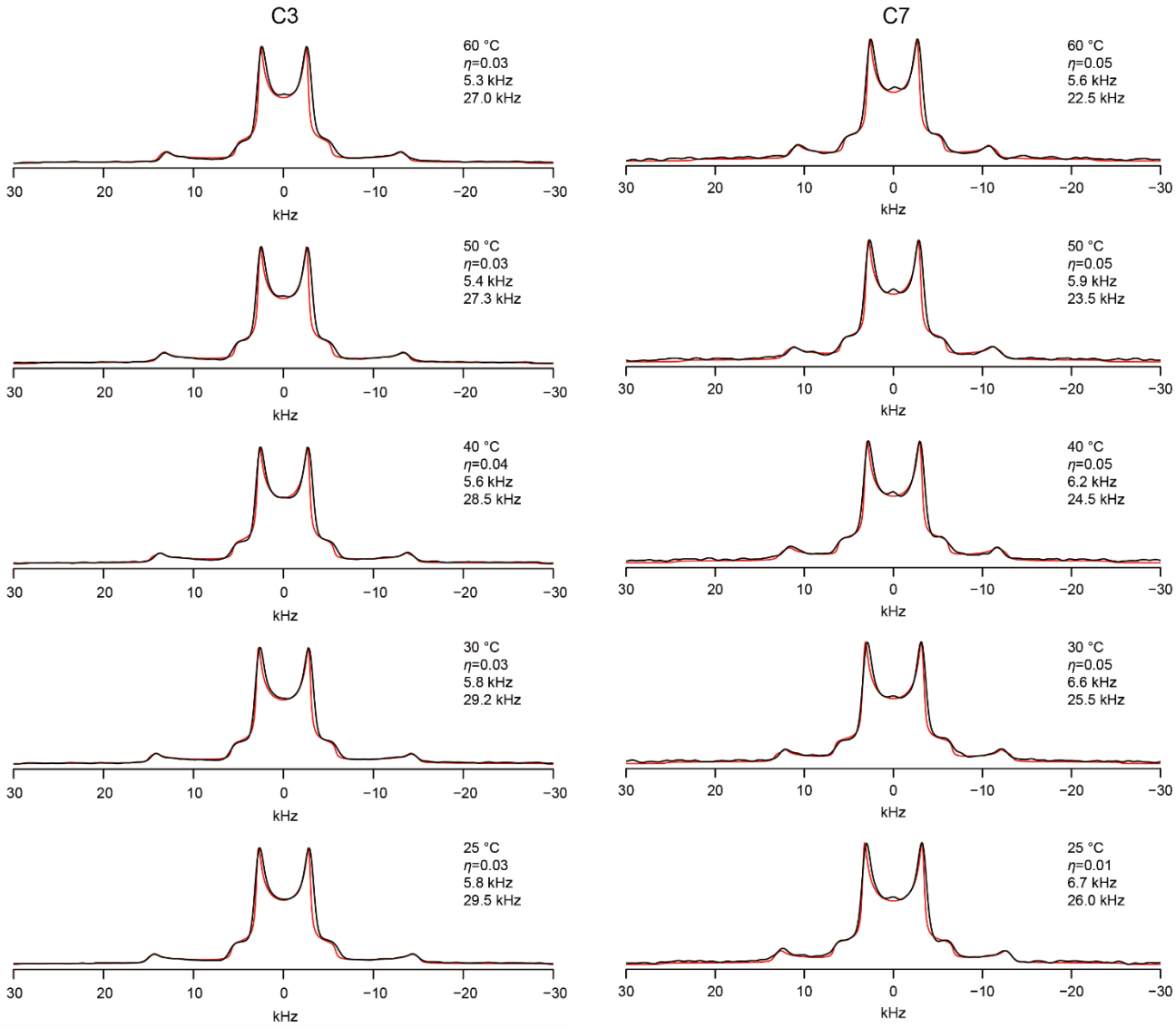

Figure S4. Experimental (black) and simulated (red) ^{2}H NMR spectra for 3'-D/CD_3 and 7'-D/CD_3 of epDPhPC at various temperatures. S_{CD} values obtained from the spectra are shown in Table 2. The quadrupole splitting width $\Delta\nu_D$ and $\Delta\nu_{CD3}$ and asymmetry parameter η were determined through spectral simulations by changing the principal elements of the quadrupole tensor, δ_{xx}, δ_{yy}, and δ_{zz}. $\Delta\nu_D = \delta_{xx} + \delta_{yy}$; $\eta = (\delta_{xx} - \delta_{yy})/\delta_{zz}$.

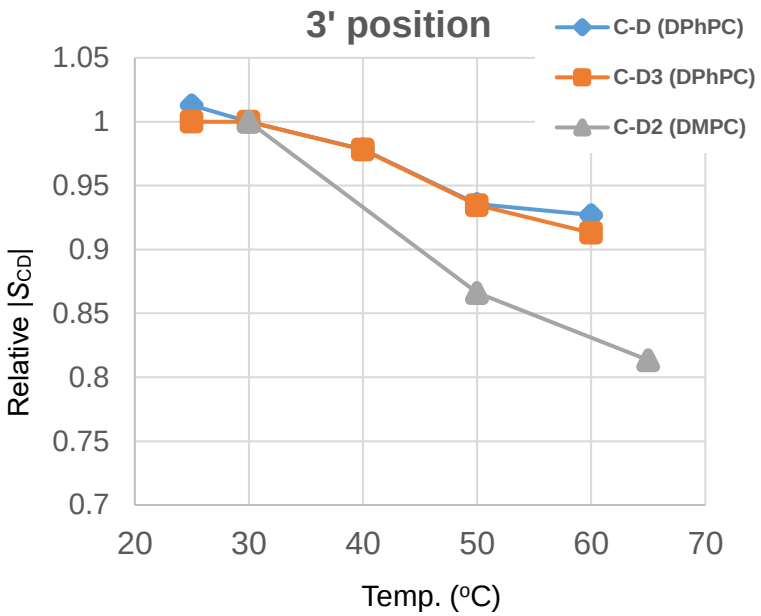

Figure S5. Temperature-dependence of relative S_{CD} values of 3'-CD_3 (orange) and 3'-CD (blue) of DPhPC, and 3'-D_2 of DMPC (gray)[2] with respect to the value at 30 °C taken as 1.0.

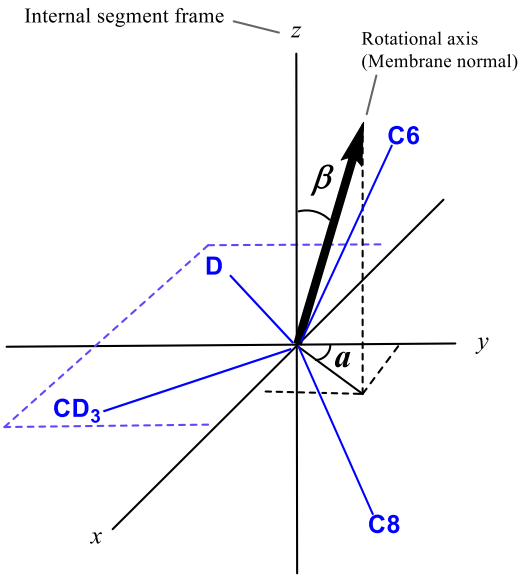

Figure S6. C7'-centered internal frame used for defining the rotational axis with angles α and β. C7'-D and C7'-CD_3 bonds of DPhPC were placed on the *xy* plane in the direction that the bisector of the C7'-D and C7'-CD_3 bonds was on the *y* axis. In the following Table S1, the plausible orientation of the C7' system was deduced from RMSD values obtained from the experimental S_{CD3}/S_{CD} ratio, 0.26, and the calculated $(3\cos^2\theta_{CD3}-1)/2 : (3\cos^2\theta_{CD}-1)/2$ ratio. Another condition was the wobbling order parameter, S_{mol}, which is equal to $-2S_{CD}$ for usual membrane phospholipids, but not applicable in this case. The possible range of S_{mol} was set to 0.46-0.70; the S_{CD} value of DPPC (or DMPC) is −0.23,[1] which can be regarded as the smallest S_{mol} values because DPPC has the average orientation $\theta_{CD} = 90°$, where $(3\cos^2\theta_{CD}-1)/2$ is equal to −0.5, and its bilayer thickness is close to that of DPhPC, which means that, if θ_{CD} deviates from 90°, S_{mol} should be larger than 0.46. We set the maximum S_{mol} somewhat higher than expected; if the average θ_{CD} is equal to 90°, the S_{mol} value of 0.70 corresponds to the $|S_{CD}|$ value of 0.35, which is exceptionally large for phospholipids in disordered phase.

Table S1. RMSD distribution chart of the difference between the experimental value (0.26) of the C-CD_3/C-D ratio and the calculated value with angles α, β; for definition of angles α, β, see Figure S6. **A**, a relevant area in this orientation analysis. **B**, the whole RMSD distribution for angles α, β. The RMSD difference from the experimental ratio (0.26) at C7' was shown for α and β angles, and the limiting condition (blue frame) of wobbling S_{mol} (0.46-0.70) was imposed. Red numbers in **A** denote α, β pairs that satisfy both conditions. The α,β pair with a red oval corresponds to the bent orientation. The bottom red one (and other pairs) turned out to be unlikely based on MD simulation that revealed the θ angle of C7'-D to be 107-108° (Table S2, Figs. S7 and S8C).

A

α° \ β°	0	5	10	15	20	25	30	35	40	45	50
5	0.050	0.051	0.054	0.059	0.067	0.078	0.095	0.118	0.154	0.212	0.315
0	0.050	0.050	0.049	0.048	0.046	0.043	0.040	0.035	0.028	0.020	0.007
−5	0.050	0.049	0.044	0.037	0.026	0.012	0.007	0.030	0.060	0.097	0.143
−10	0.050	0.047	0.040	0.027	0.009	0.015	0.046	0.082	0.126	0.176	0.234
−15	0.050	0.046	0.036	0.018	0.007	0.039	0.078	0.124	0.177	0.234	0.296
−20	0.050	0.045	0.032	0.010	0.021	0.060	0.106	0.158	0.217	0.279	0.344
−25	0.050	0.045	0.029	0.003	0.032	0.077	0.128	0.186	0.249	0.315	0.382
−30	0.050	0.044	0.026	0.002	0.042	0.090	0.146	0.209	0.276	0.345	0.414
−35	0.050	0.044	0.025	0.006	0.048	0.100	0.160	0.227	0.298	0.371	0.444
−40	0.050	0.043	0.024	0.009	0.053	0.107	0.170	0.240	0.315	0.393	0.471
−45	0.050	0.043	0.023	0.010	0.055	0.110	0.176	0.250	0.329	0.413	0.498
−50	0.050	0.043	0.024	0.009	0.054	0.110	0.178	0.255	0.340	0.431	0.526
−55	0.050	0.044	0.025	0.006	0.050	0.106	0.175	0.255	0.346	0.447	0.556
−60	0.050	0.044	0.027	0.002	0.044	0.098	0.167	0.250	0.348	0.462	0.592
−65	0.050	0.045	0.030	0.004	0.034	0.086	0.152	0.237	0.344	0.476	0.639
−70	0.050	0.046	0.033	0.011	0.022	0.068	0.131	0.215	0.330	0.488	0.709
−75	0.050	0.047	0.037	0.020	0.007	0.045	0.100	0.181	0.302	0.496	0.844
−80	0.050	0.048	0.041	0.030	0.011	0.017	0.059	0.128	0.247	0.497	1.289
−85	0.050	0.049	0.046	0.041	0.032	0.018	0.005	0.046	0.137	0.464	2.233

B

α° \ β°	0	5	10	15	20	25	30	35	40	45	50	55	60	65	70	75	80	85	90
90	0.050	0.050	0.051	0.052	0.055	0.059	0.066	0.080	0.126	2.317	0.050	0.009	0.005	0.011	0.015	0.017	0.019	0.019	0.020
85	0.050	0.051	0.056	0.065	0.079	0.105	0.155	0.283	1.130	0.686	0.287	0.192	0.151	0.128	0.115	0.106	0.101	0.098	0.097
80	0.050	0.053	0.061	0.077	0.104	0.156	0.266	0.626	7.497	0.664	0.386	0.290	0.243	0.216	0.199	0.188	0.181	0.177	0.176
75	0.050	0.054	0.065	0.088	0.129	0.209	0.397	1.250	1.999	0.672	0.446	0.354	0.306	0.277	0.259	0.247	0.240	0.236	0.234
70	0.050	0.055	0.069	0.099	0.153	0.261	0.543	2.510	1.513	0.691	0.491	0.402	0.354	0.324	0.305	0.293	0.285	0.280	0.279
65	0.050	0.055	0.073	0.108	0.174	0.309	0.689	5.409	1.375	0.716	0.528	0.441	0.392	0.362	0.342	0.329	0.321	0.316	0.315
60	0.050	0.056	0.076	0.115	0.190	0.348	0.814	12.568	1.352	0.749	0.563	0.475	0.425	0.394	0.373	0.360	0.351	0.347	0.345
55	0.050	0.057	0.078	0.121	0.202	0.374	0.891	21.295	1.401	0.791	0.599	0.507	0.455	0.422	0.400	0.386	0.377	0.372	0.371
50	0.050	0.057	0.079	0.123	0.207	0.384	0.906	14.091	1.523	0.846	0.638	0.539	0.483	0.448	0.425	0.410	0.400	0.395	0.393
45	0.050	0.057	0.079	0.124	0.207	0.379	0.861	6.847	1.757	0.922	0.683	0.573	0.511	0.472	0.447	0.431	0.421	0.415	0.413
40	0.050	0.057	0.078	0.121	0.200	0.359	0.770	3.647	2.234	1.033	0.740	0.611	0.540	0.497	0.469	0.451	0.439	0.433	0.431
35	0.050	0.056	0.077	0.117	0.189	0.328	0.657	2.150	3.534	1.213	0.818	0.658	0.573	0.523	0.491	0.470	0.457	0.450	0.447
30	0.050	0.056	0.074	0.110	0.173	0.289	0.538	1.354	17.028	1.566	0.937	0.720	0.613	0.552	0.513	0.489	0.473	0.465	0.462
25	0.050	0.055	0.071	0.102	0.154	0.246	0.426	0.882	3.911	2.579	1.154	0.815	0.667	0.587	0.538	0.508	0.489	0.479	0.476
20	0.050	0.054	0.067	0.092	0.133	0.202	0.324	0.580	1.387	41.697	1.713	0.992	0.751	0.634	0.568	0.529	0.505	0.492	0.488
15	0.050	0.053	0.063	0.082	0.111	0.158	0.235	0.375	0.679	1.784	7.313	1.487	0.922	0.715	0.611	0.553	0.519	0.502	0.496
10	0.050	0.052	0.059	0.070	0.089	0.117	0.159	0.228	0.347	0.597	1.389	28.071	1.590	0.917	0.694	0.588	0.533	0.505	0.497
5	0.050	0.051	0.054	0.059	0.067	0.078	0.095	0.118	0.154	0.212	0.315	0.541	1.362	5.522	1.100	0.684	0.541	0.481	0.464
0	0.050	0.050	0.049	0.048	0.046	0.043	0.040	0.035	0.028	0.020	0.007	0.011	0.039	0.084	0.162	0.314	0.650	1.443	2.320
−5	0.050	0.049	0.044	0.037	0.026	0.012	0.007	0.030	0.060	0.097	0.143	0.198	0.265	0.343	0.431	0.521	0.604	0.664	0.686
−10	0.050	0.047	0.040	0.027	0.009	0.015	0.046	0.082	0.126	0.176	0.234	0.297	0.365	0.436	0.505	0.568	0.619	0.652	0.664
−15	0.050	0.046	0.036	0.018	0.007	0.039	0.078	0.124	0.177	0.234	0.296	0.361	0.427	0.491	0.550	0.600	0.639	0.664	0.672
−20	0.050	0.045	0.032	0.010	0.021	0.060	0.106	0.158	0.217	0.279	0.344	0.409	0.473	0.532	0.585	0.630	0.663	0.684	0.691
−25	0.050	0.045	0.029	0.003	0.032	0.077	0.128	0.186	0.249	0.315	0.382	0.448	0.511	0.568	0.619	0.660	0.691	0.710	0.716
−30	0.050	0.044	0.026	0.002	0.042	0.090	0.146	0.209	0.276	0.345	0.414	0.482	0.546	0.604	0.654	0.694	0.725	0.743	0.749
−35	0.050	0.044	0.025	0.006	0.048	0.100	0.160	0.227	0.298	0.371	0.444	0.514	0.581	0.641	0.693	0.735	0.766	0.785	0.791
−40	0.050	0.043	0.024	0.009	0.053	0.107	0.170	0.240	0.315	0.393	0.471	0.547	0.618	0.683	0.739	0.785	0.819	0.839	0.846
−45	0.050	0.043	0.023	0.010	0.055	0.110	0.176	0.250	0.329	0.413	0.498	0.581	0.661	0.734	0.798	0.851	0.890	0.914	0.922
−50	0.050	0.043	0.024	0.009	0.054	0.110	0.178	0.255	0.340	0.431	0.526	0.621	0.714	0.801	0.879	0.943	0.992	1.022	1.033
−55	0.050	0.044	0.025	0.006	0.050	0.106	0.175	0.255	0.346	0.447	0.556	0.670	0.785	0.896	0.999	1.088	1.156	1.199	1.213
−60	0.050	0.044	0.027	0.002	0.044	0.098	0.167	0.250	0.348	0.462	0.592	0.736	0.891	1.050	1.207	1.349	1.464	1.540	1.566
−65	0.050	0.045	0.030	0.004	0.034	0.086	0.152	0.237	0.344	0.476	0.639	0.838	1.077	1.356	1.669	1.993	2.288	2.501	2.579
−70	0.050	0.046	0.033	0.011	0.022	0.068	0.131	0.215	0.330	0.488	0.709	1.032	1.522	2.313	3.693	6.370	12.293	26.282	41.753
−75	0.050	0.047	0.037	0.020	0.007	0.045	0.100	0.181	0.302	0.496	0.844	1.606	4.377	18.845	3.929	2.526	2.042	1.841	1.784
−80	0.050	0.048	0.041	0.030	0.011	0.017	0.059	0.128	0.247	0.497	1.289	28.170	1.690	1.017	0.794	0.688	0.633	0.605	0.597
−85	0.050	0.049	0.046	0.041	0.032	0.018	0.005	0.046	0.137	0.464	2.233	0.506	0.338	0.277	0.246	0.229	0.219	0.214	0.212

1<RMSD　0.01<RMSD<0.05　RMSD<0.009　0.46<S_{mol}<0.70

Table S2. Comparison of NMR and MD results for orientation of C-D bonds of DPhPC[a]

Postn.	NMR, *sn*-2 (30 °C)			MD, *sn*-1			MD, *sn*-2		
	bent S_{mol}[c]	linear S_{mol}[c]	bent angle θ	bent S_{mol}[c]	linear S_{mol}[c]	bent angle θ	bent S_{mol}[c]	linear S_{mol}[c]	bent angle θ
3’	(0.661)[b]	0.466	(108)[b]	0.49	0.35	-	0.66	0.47	-[b]
7’	0.571	0.408	108	0.52	0.37	73 [d]	0.55	0.39	107

[a] see Table 3 for other parameters; [b] C3’-D partly takes the 40°-upward bent orientation (see Fig. S10); [c]S_{mol} values were obtained by dividing the S_{CD} values (Tables 2 and 5) by $(3\cos^2\theta - 1)/2$. [d]θ angle was deduced for the upward bent orientation.

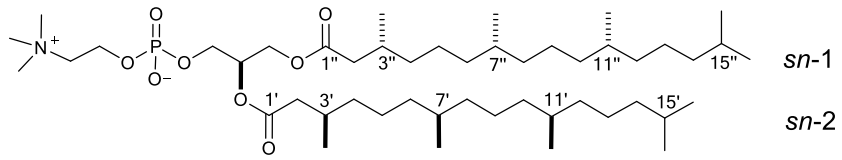

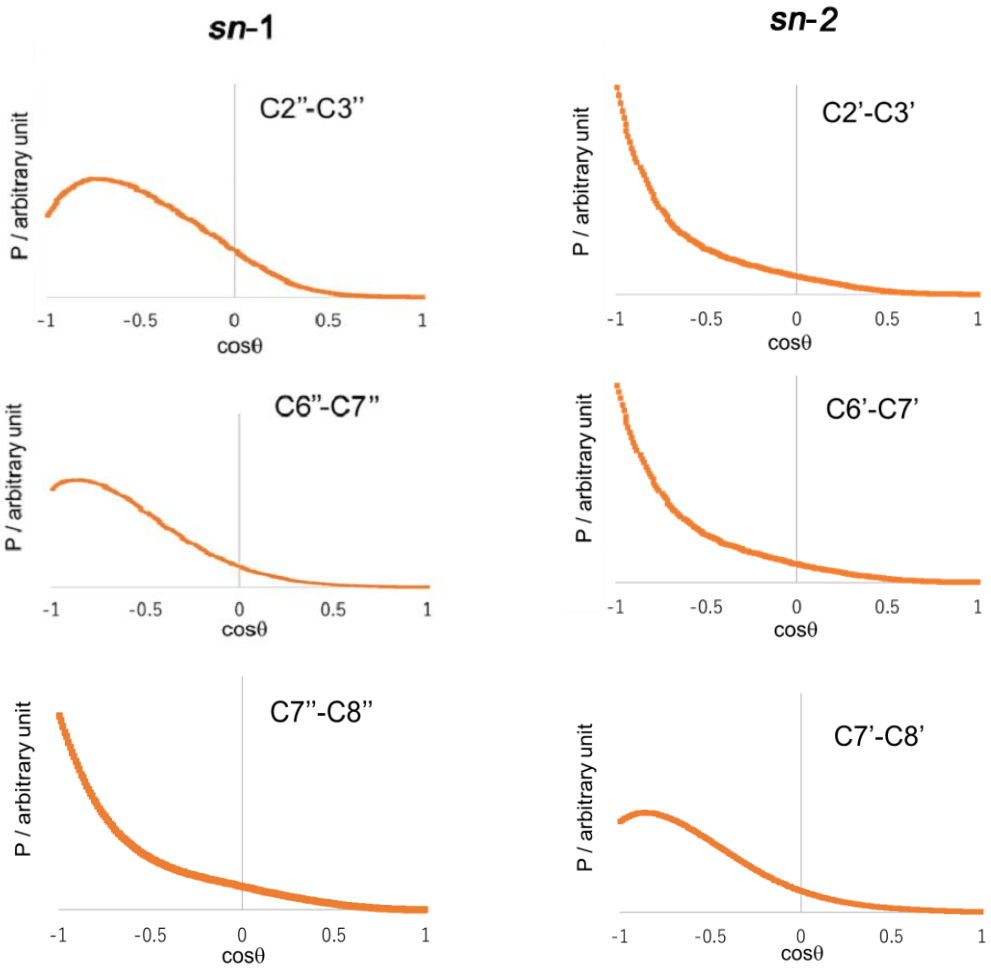

Figure S7. Angle distribution between the C2”-C3” (C6”-C7”) bond of *sn*-1 and the bilayer normal, and between the C2’-C3’ (C6’-C7’) bond of *sn*-2 and the bilayer normal, derived from MD calculation. The average orientation of the C6”-C7” bond (*sn*-1) significantly tilts from -180° while

that of the C6'-C7' bond (*sn*-2) is directed parallel to the bilayer normal. Similar angle distributions are observed for the C7''-C8'' and C7'-C8' bonds but in the opposite way. This alternating orientation change is due to the upward and downward bent orientations of *sn*-1 and *sn*-2 chains, respectively (Fig. 6b).

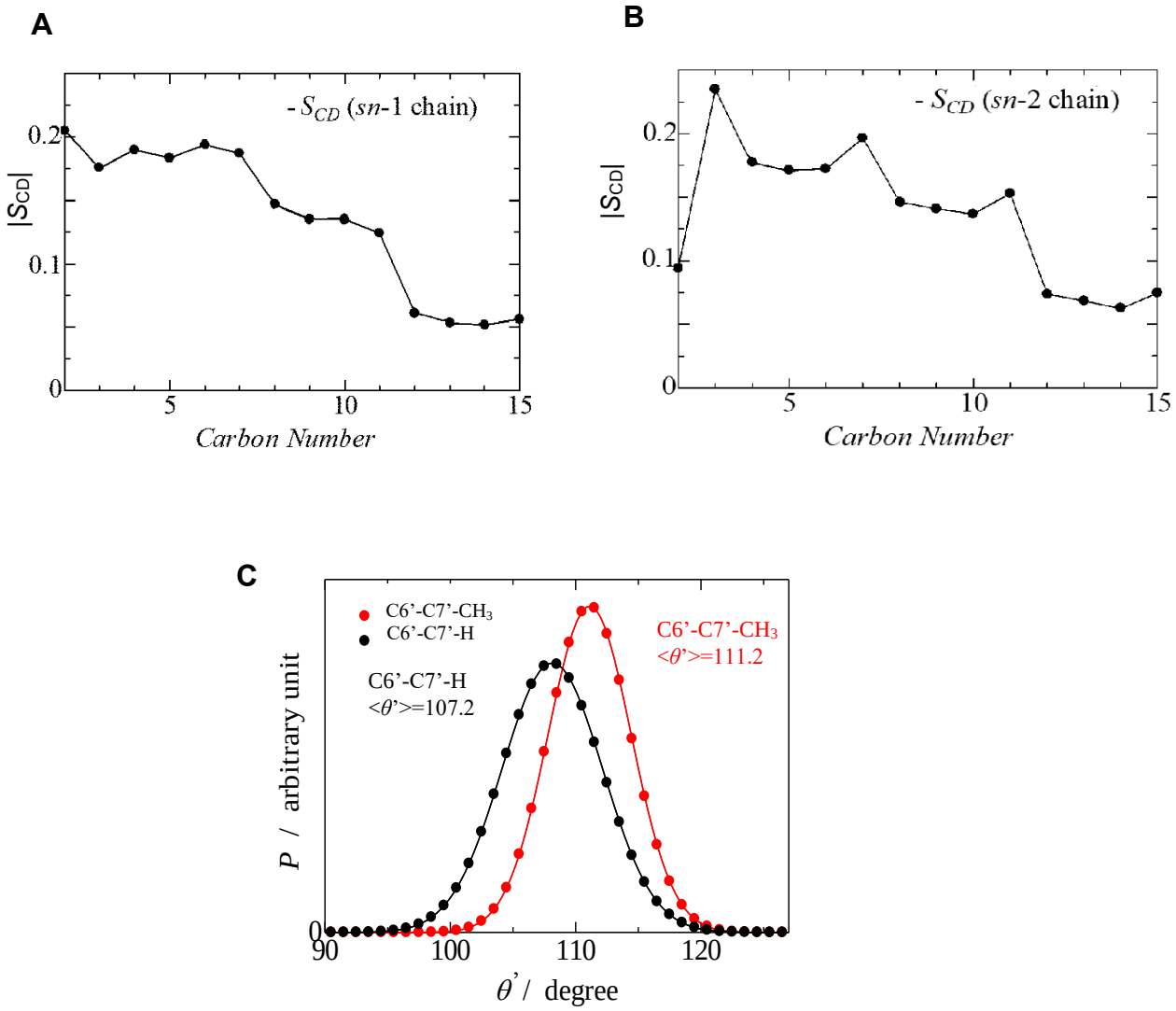

,

Figure S8. Order profiles of DPhPC. **A**, **B**, S_{CD} values of C-H bond in sn-1 and sn-2 chains of DPhPC. **C**, Distributions of angule θ' which is the bond angles of C6'-C7'-D and C6'-C7'-CD_3, showing Gauss curves, where dots and lines denote the bond angles from MD calculations and standard Gauss curves, respectively. In the bent orientation, θ' is equal to the average angle θ because the C6'-C7' bond is in parallel to the rotational axis (Table S1 and Figure 4).

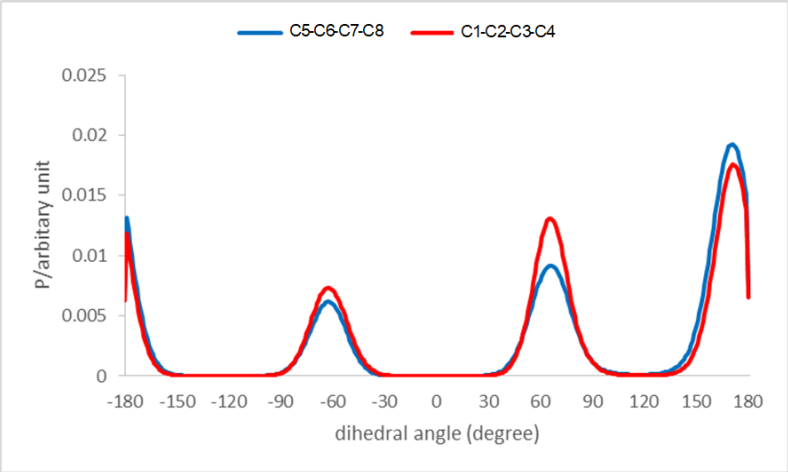

anti : $-180^{o} < \theta < -120^{o}$, $120^{o} < \theta < 180^{o}$

gauche + : $0^{o} < \theta < 120^{o}$

gauche − : $-120^{o} < \theta < 0^{o}$

Figure S9. Distribution of dihedral angles C1' − C2' − C3' − C4' and C5' − C6' − C7' − C8' of the *sn*-2 phytanyl chain of DPhPC.

Table S3. Conformational populations around the C3' and C7' positions

Postn	conformation (%)		
	anti	*g*+	*g*-
3	47	33	20
7	57	27	16

The conformation at C3' and C7' positions of DPhPC is shown as the rotational conformers anti, gauche^{+}, and gauche^{-} with respect to C1' − C2' − C3' − C4' and C5' − C6' − C7' − C8', respectively.

In order to obtain the $S_{CD(CD3)}/S_{CD(D)}$ ratio for each of the linear, bent and upward bent structures, the rotational conformations at the C3 and C7 positions are calculated (Table S3). In the case of the linear and the 40^{o} upward-bent structure, the angle between the membrane normal and the CD (or C-CD_3) bond differs among *anti*, *gauche* +, and *gauche* − conformations (Figure 5). To calculate the $S_{CD(CD3)}/S_{CD(D)}$ ratios, the abundance ratios of *anti*, *gauche* +, and *gauche* − were obtained as shown in Table S3. S_{CD} values were directly calculated from the populations of the rotational conformation and the orientation angles, the $|S_{CD\,(CD3)}/S_{CD\,(CD)}|$ ratios were obtained for the C3 and C7 positions as shown in Table 3. On the other hand, in the case of the usual bent structures, the angle between the membrane normal and the CD, C-CD_3 bond is constant regardless of the *anti*, *gauche* +, or *gauche* − in the

rotational conformation to be $|S_{CD\,(CD3)}/S_{CD\,(CD)}|\approx 0.26$.

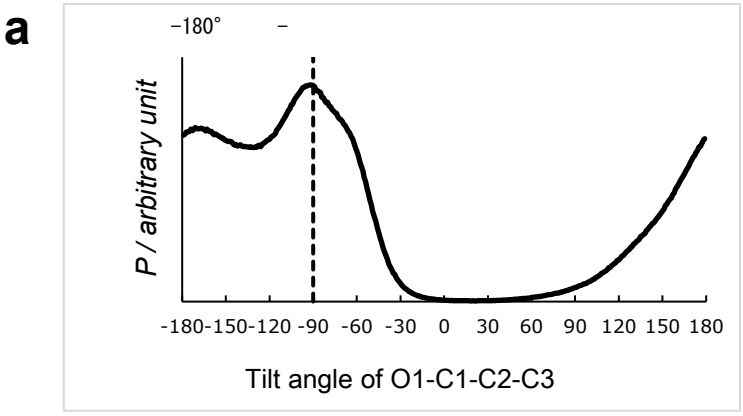

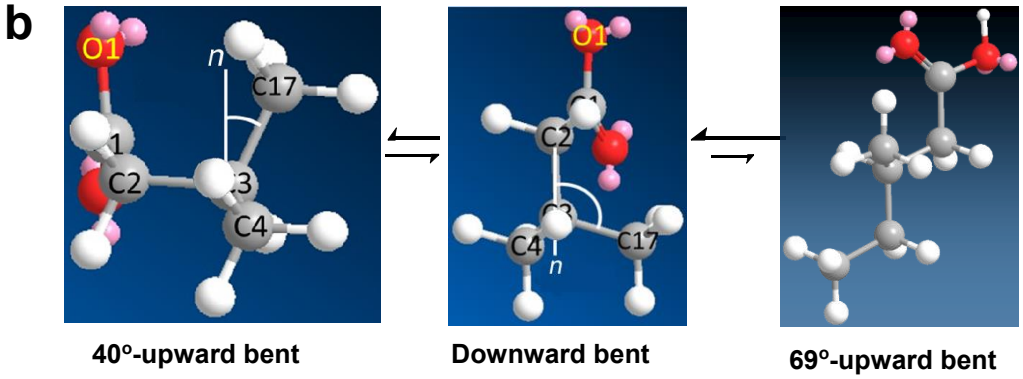

Figure S10. Tilt angle distribution of O1'-C1'-C2'-C3' of *sn*-2 chain of DPhPC deduced by MD calculation (**a**). Higher stereochemical repulsion between CH_3 (labeled as C17) and C1=O in the usual bent conformation (**b, right**) causes the 40°-methyl-upward bent conformation (**b, left)** at the C3' position of DPhPC. The angle between the C3-CH_3(C17) bond and the membrane normal is shown in Fig. 5b, in which the 40°-methyl-upward orientation appeared to be the second most stable conformation.

The C3 position of DPhPC is significantly different from that of PGP-Me with respect to the orientation angle of the methyl group. Although both of the lipids take downward bent structure at the C3 position as a main orientation, ether-type PGP-Me has the second bent structure with 3-CH_3 group facing upward at around 66°($\cos\theta$ = 0.41) whereas the 3-CH_3 of DPhPC shows more profoundly upward direction with around 40°($\cos\theta$ = 0.77) (Fig. 6b). The reason why such a structure was found in DPhPC may be due to the steric repulsion between the carbonyl oxygen and the methyl group in the usual bent conformation (Figure S10).

In order to confirm that the 40°-methyl-upward orientation of the 3-methyl group of DPhPC was due to steric repulsion between the carbonyl oxygen and the methyl group, we examined the MD simulation results more in detail. As shown in Figure S10a, the tilt angle of 90° about O1-C1-C2-C3 turned out to be stable for DPhPC in bilayers. This structure was markedly different from the conformation of PGP-Me, where the upward bent conformation with the orientation at θ=69° was relatively stable at the C3 position. Thus, the structural difference between DPhPC and PGP-Me is the main cause to stabilize the 40°-methyl-upward orientation, implying that the steric repulsion between the carbonyl oxygen and the methyl group should be the main driving force of this orientation. The temperature-dependent change of $\Delta\nu$ values in Fig. 3 indicates that the thermal stability of DPhPC at the C3 position is lower than that of PGP-Me (ref. 22). The 40°-methyl-upward orientation occurring in DPhPC may loosen the chain packing to slightly decrease the thermal stability of phytanoyl chains.

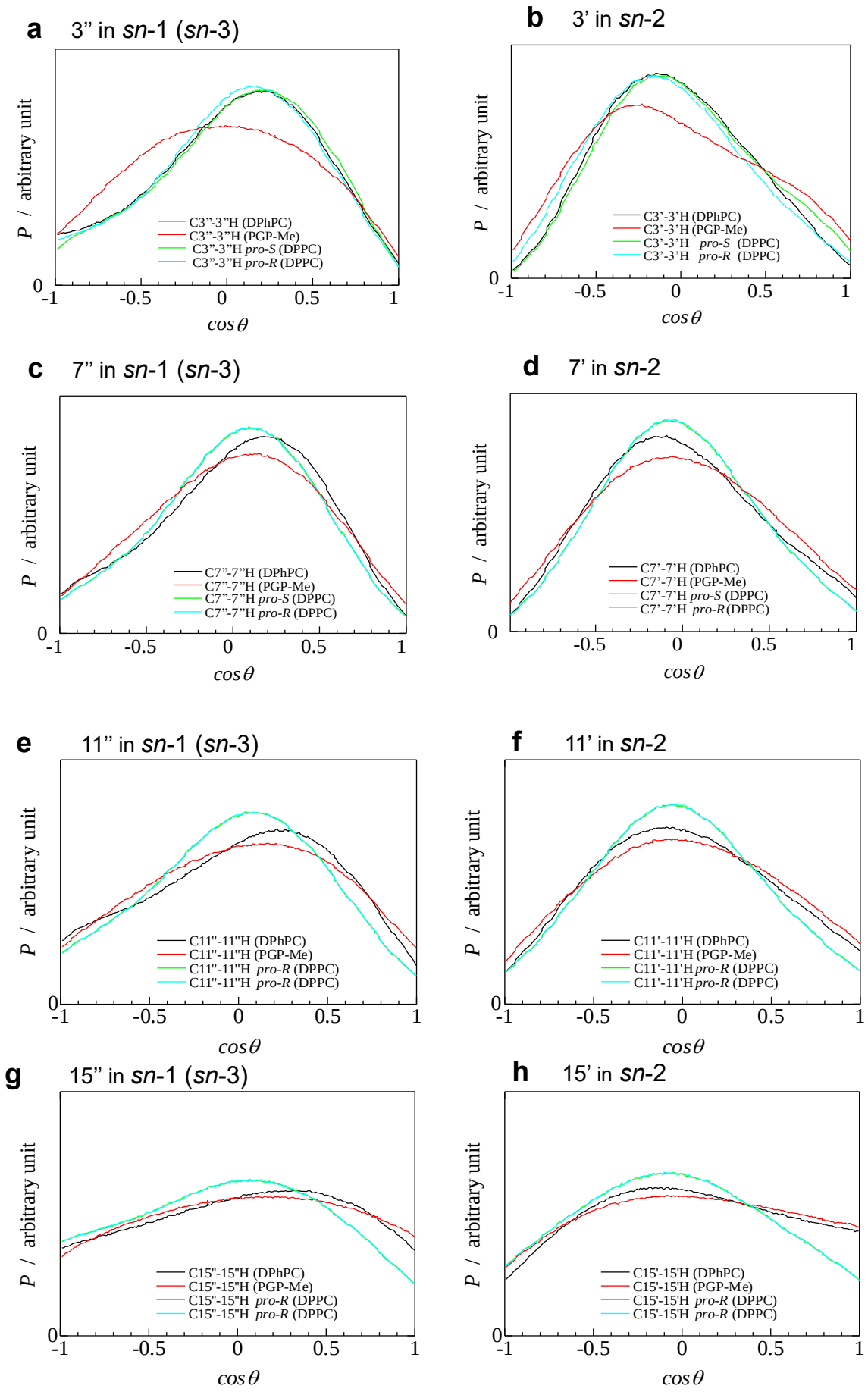
a
3” in sn-1 (sn-3)
P / arbitrary unit
cos θ
C3”-3”H (DPhPC)
C3”-3”H (PGP-Me)
C3”-3”H pro-S (DPPC)
C3”-3”H pro-R (DPPC)
b
3’ in sn-2
C3’-3’H (DPhPC)
C3’-3’H (PGP-Me)
C3’-3’H pro-S (DPPC)
C3’-3’H pro-R (DPPC)
c
7” in sn-1 (sn-3)
C7”-7”H (DPhPC)
C7”-7”H (PGP-Me)
C7”-7”H pro-S (DPPC)
C7”-7”H pro-R (DPPC)
d
7’ in sn-2
C7’-7’H (DPhPC)
C7’-7’H (PGP-Me)
C7’-7’H pro-S (DPPC)
C7’-7’H pro-R (DPPC)
e
11” in sn-1 (sn-3)
C11”-11”H (DPhPC)
C11”-11”H (PGP-Me)
C11”-11”H pro-R (DPPC)
C11”-11”H pro-R (DPPC)
f
11’ in sn-2
C11’-11’H (DPhPC)
C11’-11’H (PGP-Me)
C11’-11’H pro-R (DPPC)
C11’-11’H pro-R (DPPC)
g
15” in sn-1 (sn-3)
C15”-15”H (DPhPC)
C15”-15”H (PGP-Me)
C15”-15”H pro-R (DPPC)
C15”-15”H pro-R (DPPC)
h
15’ in sn-2
C15’-15’H (DPhPC)
C15’-15’H (PGP-Me)
C15’-15’H pro-R (DPPC)
C15’-15’H pro-R (DPPC)

Figure S11. Angle distribution between the methyl branching bond of the *sn*-1 and *sn*-2 chains of DPhPC and the bilayer normal derived from MD calculations. C3''—H (**a**), C3'—H (**b**), C7''—H (**c**), C7'—H (**d**), C11''—H (**e**), C11'—H (**f**), C15''—H (**g**), and C15'—H (**h**), in comparison with the corresponding bonds in the *sn*-3 and *sn-1* chains of PGPMe (ref. 22) and *sn*-1 and *sn*-2 chains of DPPC.

VI. Molecular dynamics (MD) simulations

Here we provide several basic structural quantities obtained from 1μs-MD simulation of DPhPC bilayer. Figure S12 plots lamellar repeat spacing, L_z, and molecular area of DPhPC. The averaged molecular area over the last 900 ns was 78.8 Å^2 (at 298K; simulation temperature), which is in good agreement with experimental data of 78.0 Å^2 at 293K and 80.6 Å^2 at 303K[3]. Figure S13 plots membrane thickness as represented by d_{PP}; phosphate-phosphate distance across the membrane. The averaged d_{PP} was 37.2 Å, which slightly overestimated the experimental value of 36.3±0.7 Å at 293K[3].

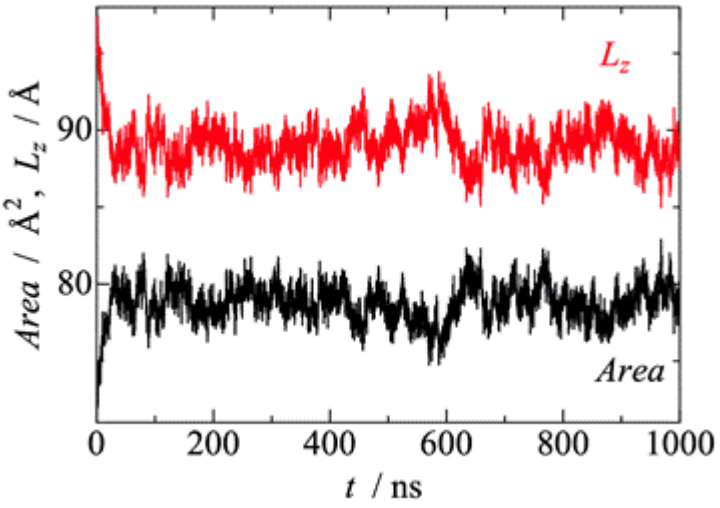

Figure S12. Time evolution of the molecular area of epDPhPC and lamellar repeat spacing (*Lz*) during 1 μs-MD simulation.

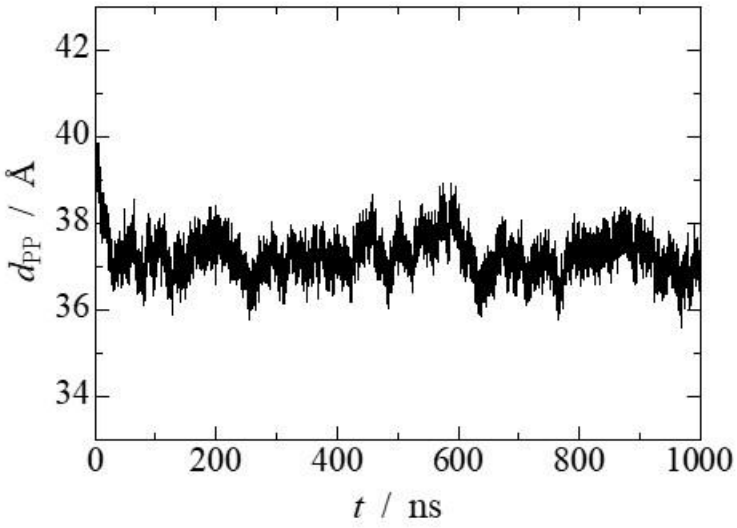

Figure S13. Time evolution of the membrane thickness (d_{PP}; distance between two phosphorus position in upper and lower leaflets) during 1 μs-MD simulation.

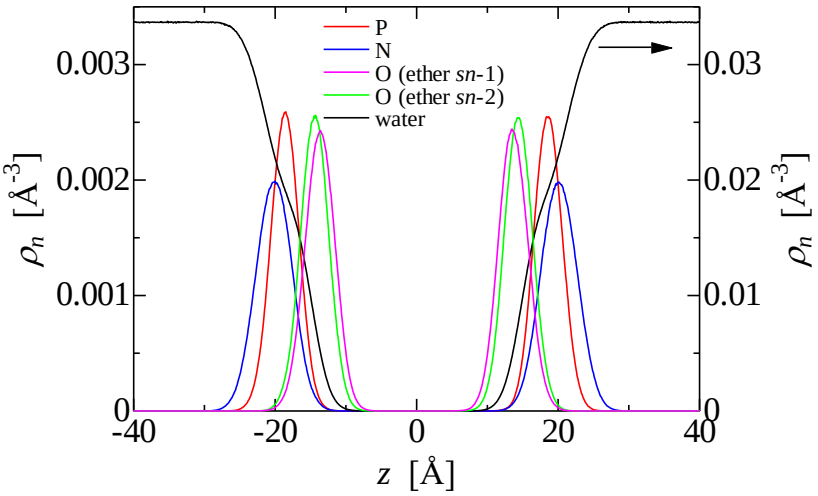

Figure S14. Number density profiles for several atoms of lipid and water molecule calculated from the last 900 ns -MD trajectory.

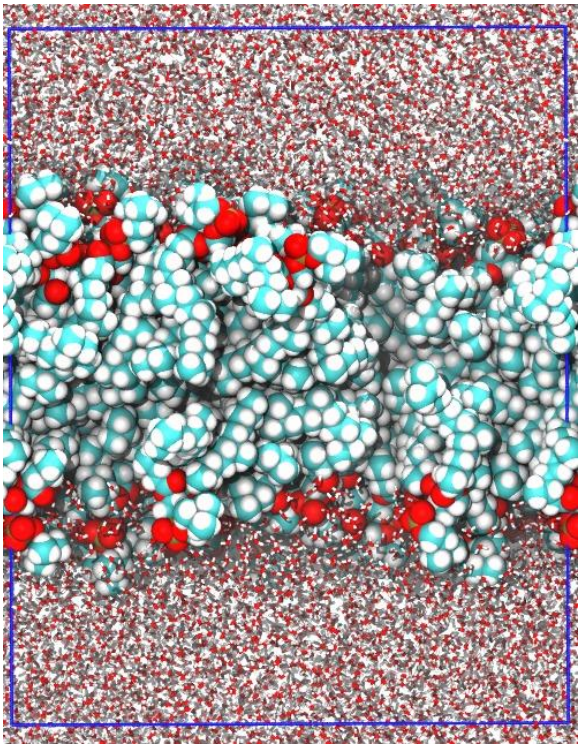

Figure S15. A snapshot of DPhPC bilayer from MD simulation.

VII. References

1) Marsh, D., Watts, A., Smith, I. C. P. (1983) Dynamic structure and phase behavior of dimyristoylphosphatidylethanolamine bilayers studied by deuterium nuclear magnetic resonance. *Biochemistry, 22*, 3023-3026.
2) Petrache, H. I., Dodd, S. W., and Brown, M. F. (2000) Area per lipid and acyl length distributions in fluid phosphatidylcholines determined by ^{2}H NMR spectroscopy. *Biophys. J. 79*, 3172–3192.
3) Kucerka, N., Nieh, M.-P., Katsaras, J. (2011) Fluid phase lipid areas and bilayer thicknesses of commonly used phosphatidylcholines as a function of temperature. *BBA-Biomembrane, 1808*, 2761-2771.

VIII. ^{1}H and ^{13}C NMR spectra of synthetic products

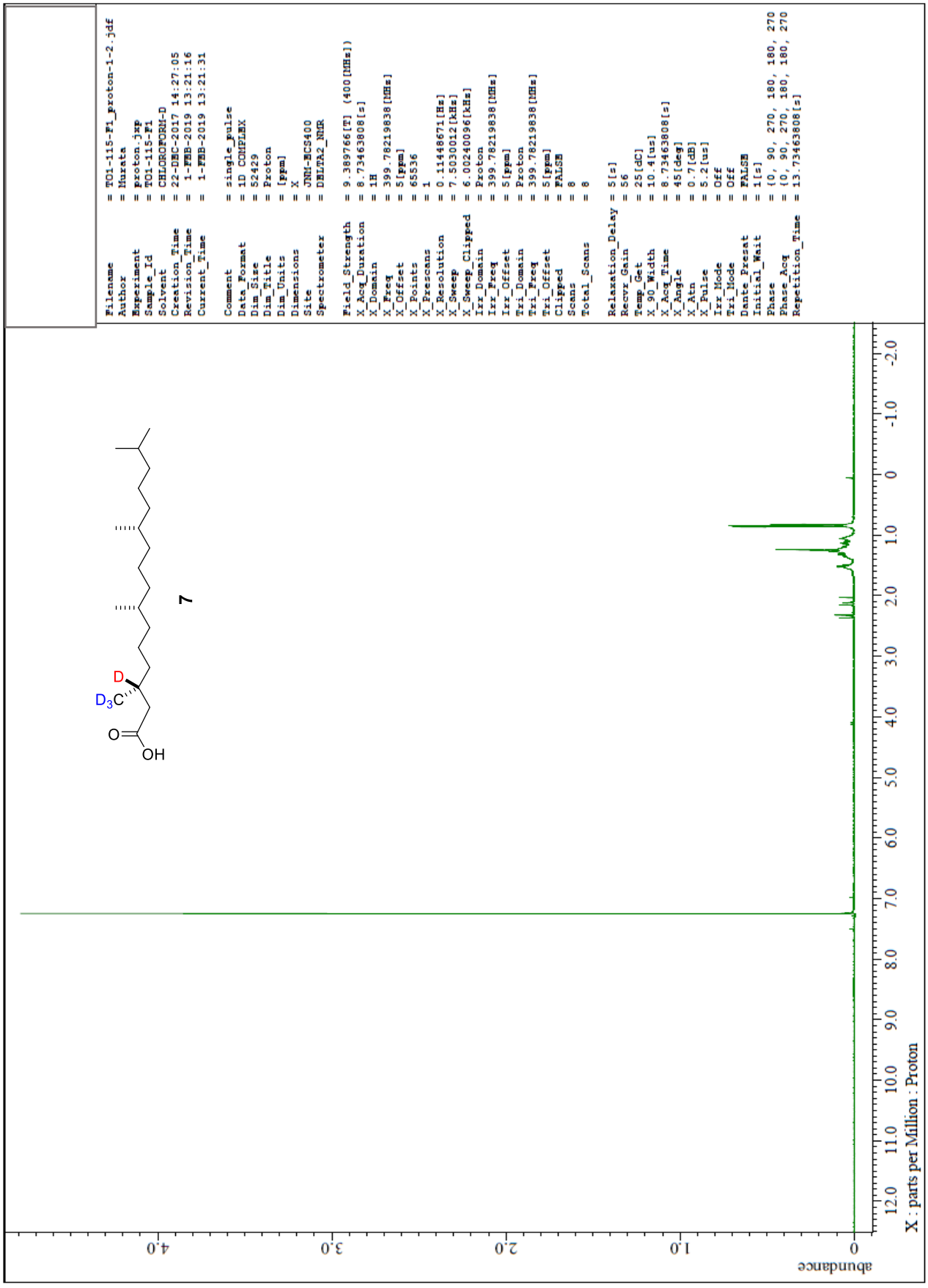

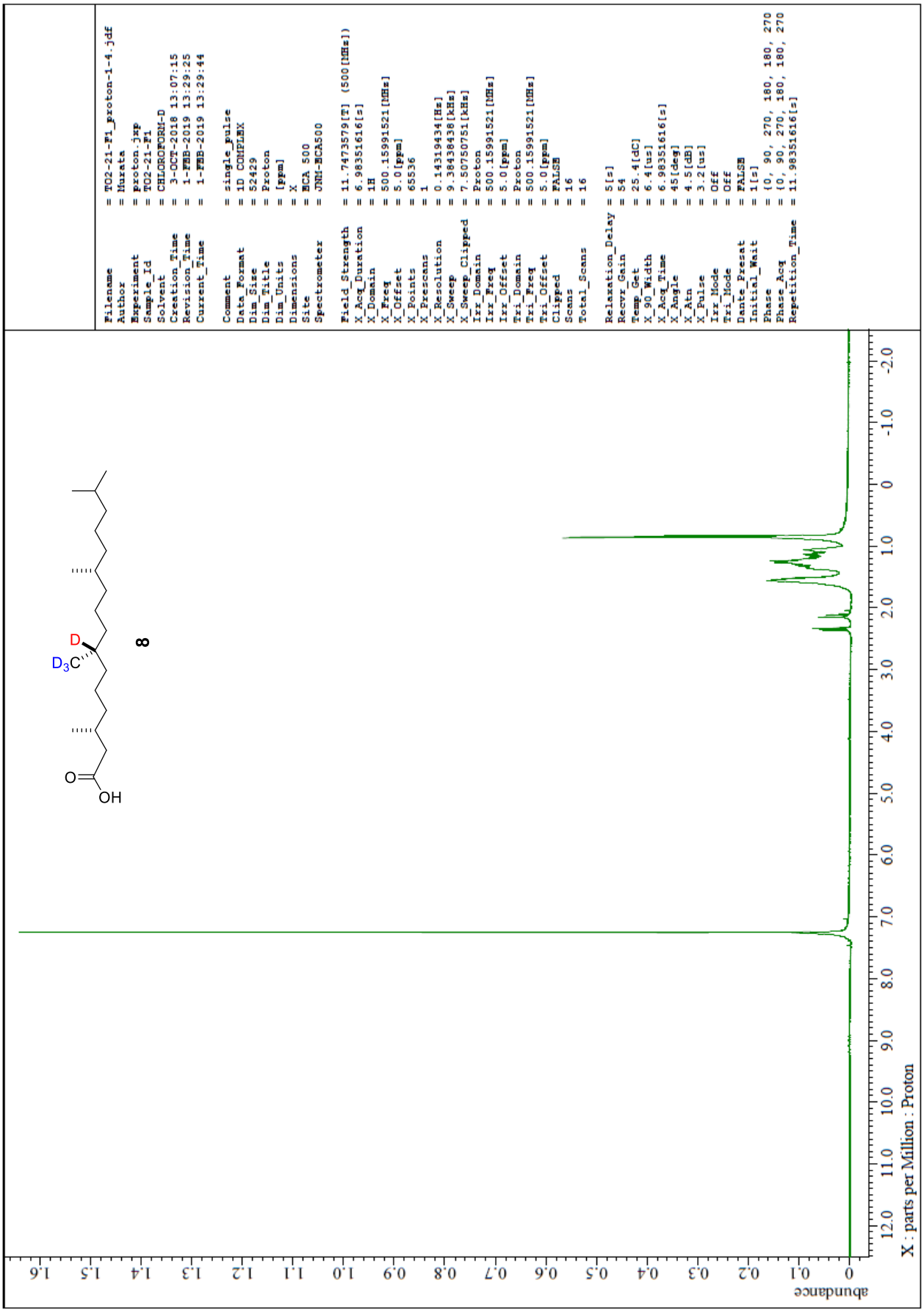
Filename = TO2-21-F1_proton-1-4.jdf
Author = Murata
Experiment = proton.jxp
Sample_Id = TO2-21-F1
Solvent = CHLOROFORM-D
Creation_Time = 3-OCT-2018 13:07:15
Revision_Time = 1-FEB-2019 13:29:25
Current_Time = 1-FEB-2019 13:29:44
Comment = single_pulse
Data_Format = 1D COMPLEX
Dim_Size = 52429
Dim_Title = Proton
Dim_Units = [ppm]
Dimensions = X
Site = BCA 500
Spectrometer = JNM-BCA500
Field_Strength = 11.74735579[T] (500[MHz])
X_Acq_Duration = 6.98351616[s]
X_Domain = 1H
X_Freq = 500.15991521[MHz]
X_Offset = 5.0[ppm]
X_Points = 65536
X_Prescans = 1
X_Resolution = 0.14319434[Hz]
X_Sweep = 9.38438438[kHz]
X_Sweep_Clipped = 7.50750751[kHz]
Irr_Domain = Proton
Irr_Freq = 500.15991521[MHz]
Irr_Offset = 5.0[ppm]
Tri_Domain = Proton
Tri_Freq = 500.15991521[MHz]
Tri_Offset = 5.0[ppm]
Clipped = FALSE
Scans = 16
Total_Scans = 16
Relaxation_Delay = 5[s]
Recvr_Gain = 54
Temp_Get = 25.4[dC]
X_90_Width = 6.4[us]
X_Acq_Time = 6.98351616[s]
X_Angle = 45[deg]
X_Atn = 4.5[dB]
X_Pulse = 3.2[us]
Irr_Mode = Off
Tri_Mode = Off
Dante_Presat = FALSE
Initial_Wait = 1[s]
Phase = (0, 90, 270, 180, 180, 270
Phase_Acq = (0, 90, 270, 180, 180, 270
Repetition_Time = 11.98351616[s]
D
D3C
O
OH
8
abundance
X : parts per Million : Proton

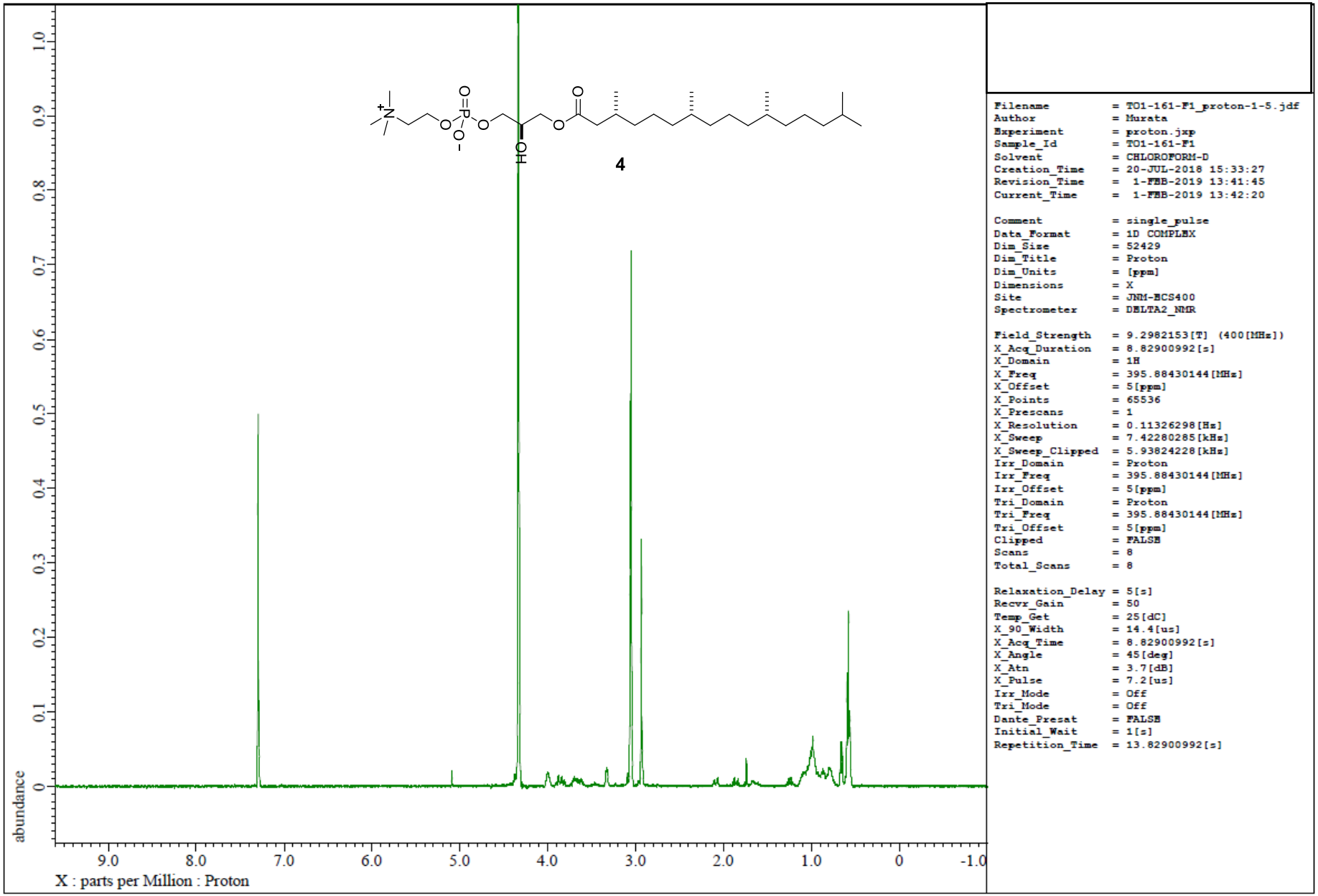


```
Filename          = TO1-161-F1_proton-1-5.jdf
Author            = Murata
Experiment        = proton.jxp
Sample_Id         = TO1-161-F1
Solvent           = CHLOROFORM-D
Creation_Time     = 20-JUL-2018 15:33:27
Revision_Time     =  1-FEB-2019 13:41:45
Current_Time      =  1-FEB-2019 13:42:20

Comment           = single_pulse
Data_Format       = 1D COMPLEX
Dim_Size          = 52429
Dim_Title         = Proton
Dim_Units         = [ppm]
Dimensions        = X
Site              = JNM-ECS400
Spectrometer      = DELTA2_NMR

Field_Strength    = 9.2982153[T] (400[MHz])
X_Acq_Duration    = 8.82900992[s]
X_Domain          = 1H
X_Freq            = 395.88430144[MHz]
X_Offset          = 5[ppm]
X_Points          = 65536
X_Prescans        = 1
X_Resolution      = 0.11326298[Hz]
X_Sweep           = 7.42280285[kHz]
X_Sweep_Clipped   = 5.93824228[kHz]
Irr_Domain        = Proton
Irr_Freq          = 395.88430144[MHz]
Irr_Offset        = 5[ppm]
Tri_Domain        = Proton
Tri_Freq          = 395.88430144[MHz]
Tri_Offset        = 5[ppm]
Clipped           = FALSE
Scans             = 8
Total_Scans       = 8

Relaxation_Delay = 5[s]
Recvr_Gain        = 50
Temp_Get          = 25[dC]
X_90_Width        = 14.4[us]
X_Acq_Time        = 8.82900992[s]
X_Angle           = 45[deg]
X_Atn             = 3.7[dB]
X_Pulse           = 7.2[us]
Irr_Mode          = Off
Tri_Mode          = Off
Dante_Presat      = FALSE
Initial_Wait      = 1[s]
Repetition_Time   = 13.82900992[s]
```

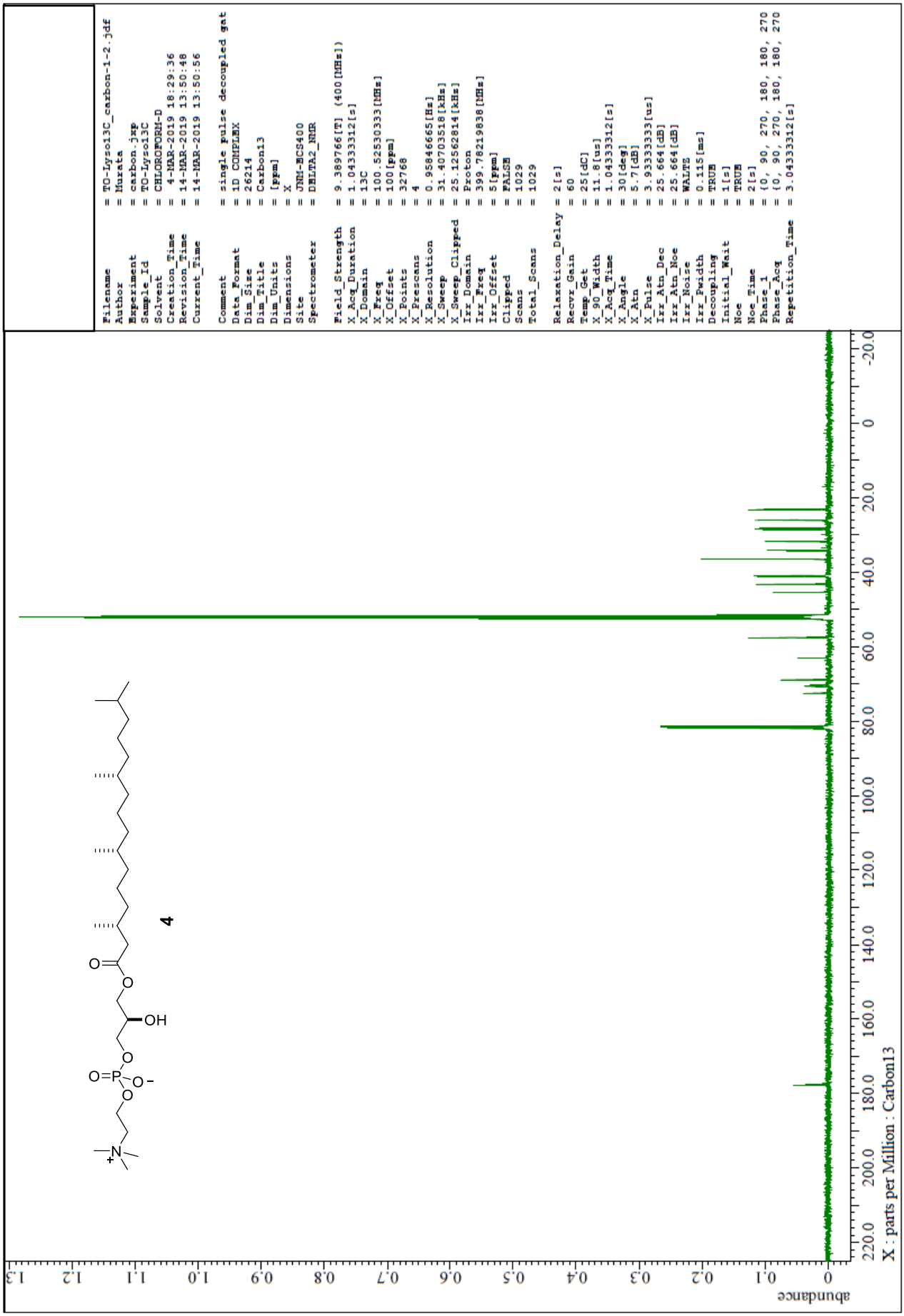
Filename = TO-Lyso13C_carbon-1-2.jdf
Author = Murata
Experiment = carbon.jxp
Sample_Id = TO-Lyso13C
Solvent = CHLOROFORM-D
Creation_Time = 4-MAR-2019 18:29:36
Revision_Time = 14-MAR-2019 13:50:48
Current_Time = 14-MAR-2019 13:50:56
Comment = single pulse decoupled gat
Data_Format = 1D COMPLEX
Dim_Size = 26214
Dim_Title = Carbon13
Dim_Units = [ppm]
Dimensions = X
Site = JNM-ECS400
Spectrometer = DELTA2_NMR
Field_Strength = 9.389766[T] (400[MHz])
X_Acq_Duration = 1.043333312[s]
X_Domain = 13C
X_Freq = 100.52530333[MHz]
X_Offset = 100[ppm]
X_Points = 32768
X_Prescans = 4
X_Resolution = 0.95846665[Hz]
X_Sweep = 31.407033518[kHz]
X_Sweep_Clipped = 25.125628214[kHz]
Irr_Domain = Proton
Irr_Freq = 399.78219838[MHz]
Irr_Offset = 5[ppm]
Clipped = FALSE
Scans = 1029
Total_Scans = 1029
Relaxation_Delay = 2[s]
Recvr_Gain = 60
Temp_Get = 25[dC]
X_90_Width = 11.8[us]
X_Acq_Time = 1.043333312[s]
X_Angle = 30[deg]
X_Atn = 5.7[dB]
X_Pulse = 3.933333333[us]
Irr_Atn_Dec = 25.664[dB]
Irr_Atn_Noe = 25.664[dB]
Irr_Noise = WALTZ
Irr_Pwidth = 0.115[ms]
Decoupling = TRUE
Initial_Wait = 1[s]
Noe = TRUE
Noe_Time = 2[s]
Phase_1 = (0, 90, 270, 180, 180, 270
Phase_Acq = (0, 90, 270, 180, 180, 270
Repetition_Time = 3.043333312[s]
4
O
O
OH
O
O=P
O
O -
O
N+
abundance
0.1
0.2
0.3
0.4
0.5
0.6
0.7
0.8
0.9
1.0
1.1
1.2
1.3
220.0
200.0
180.0
160.0
140.0
120.0
100.0
80.0
60.0
40.0
20.0
0
-20.0
X : parts per Million : Carbon13

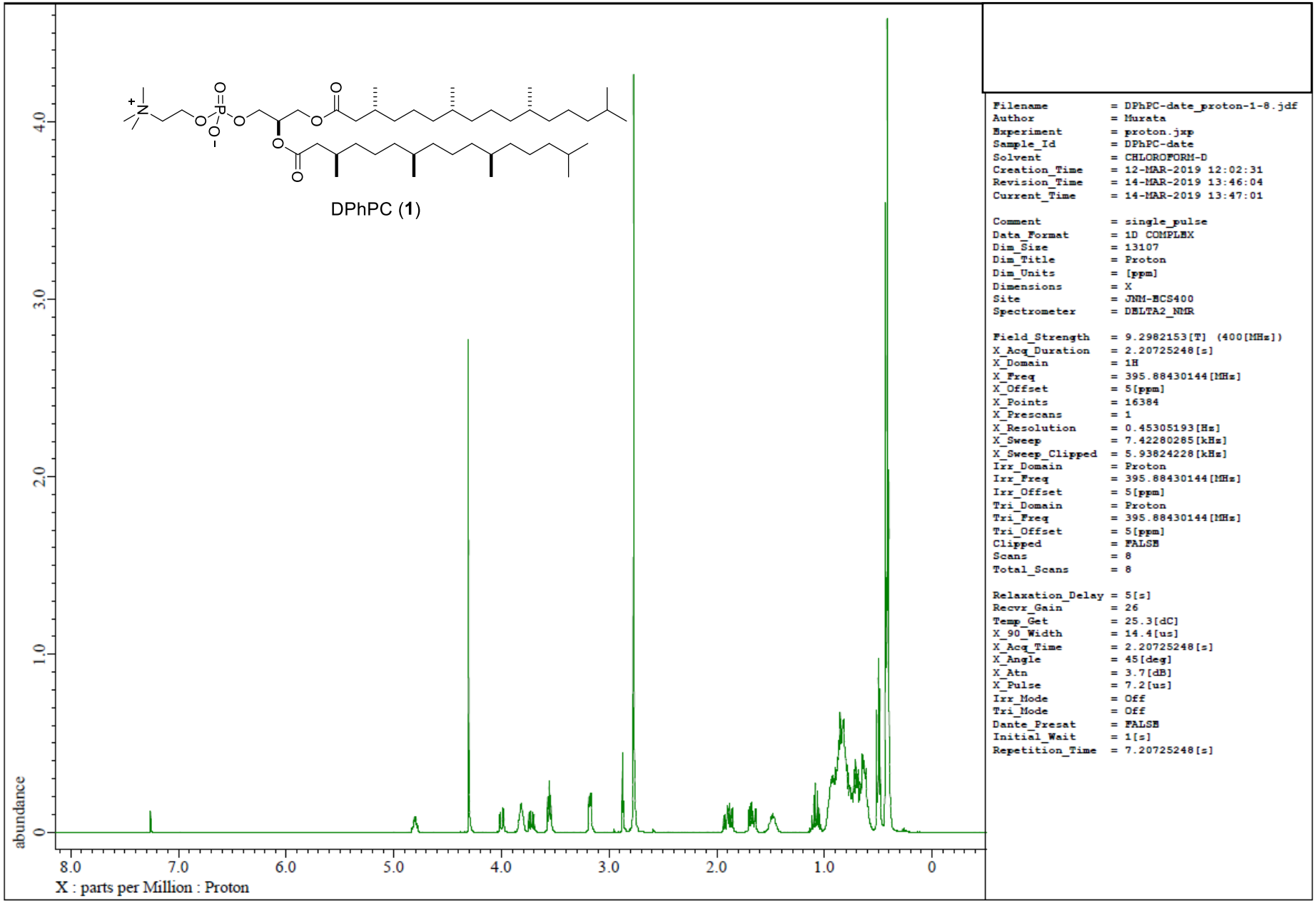
DPhPC (1)
abundance
X : parts per Million : Proton
8.0
7.0
6.0
5.0
4.0
3.0
2.0
1.0
0
Filename = DPhPC-date_proton-1-8.jdf
Author = Murata
Experiment = proton.jxp
Sample_Id = DPhPC-date
Solvent = CHLOROFORM-D
Creation_Time = 12-MAR-2019 12:02:31
Revision_Time = 14-MAR-2019 13:46:04
Current_Time = 14-MAR-2019 13:47:01
Comment = single_pulse
Data_Format = 1D COMPLEX
Dim_Size = 13107
Dim_Title = Proton
Dim_Units = [ppm]
Dimensions = X
Site = JNM-ECS400
Spectrometer = DELTA2_NMR
Field_Strength = 9.2982153[T] (400[MHz])
X_Acq_Duration = 2.20725248[s]
X_Domain = 1H
X_Freq = 395.88430144[MHz]
X_Offset = 5[ppm]
X_Points = 16384
X_Prescans = 1
X_Resolution = 0.45305193[Hz]
X_Sweep = 7.42280285[kHz]
X_Sweep_Clipped = 5.93824228[kHz]
Irr_Domain = Proton
Irr_Freq = 395.88430144[MHz]
Irr_Offset = 5[ppm]
Tri_Domain = Proton
Tri_Freq = 395.88430144[MHz]
Tri_Offset = 5[ppm]
Clipped = FALSE
Scans = 8
Total_Scans = 8
Relaxation_Delay = 5[s]
Recvr_Gain = 26
Temp_Get = 25.3[dC]
X_90_Width = 14.4[us]
X_Acq_Time = 2.20725248[s]
X_Angle = 45[deg]
X_Atn = 3.7[dB]
X_Pulse = 7.2[us]
Irr_Mode = Off
Tri_Mode = Off
Dante_Presat = FALSE
Initial_Wait = 1[s]
Repetition_Time = 7.20725248[s]

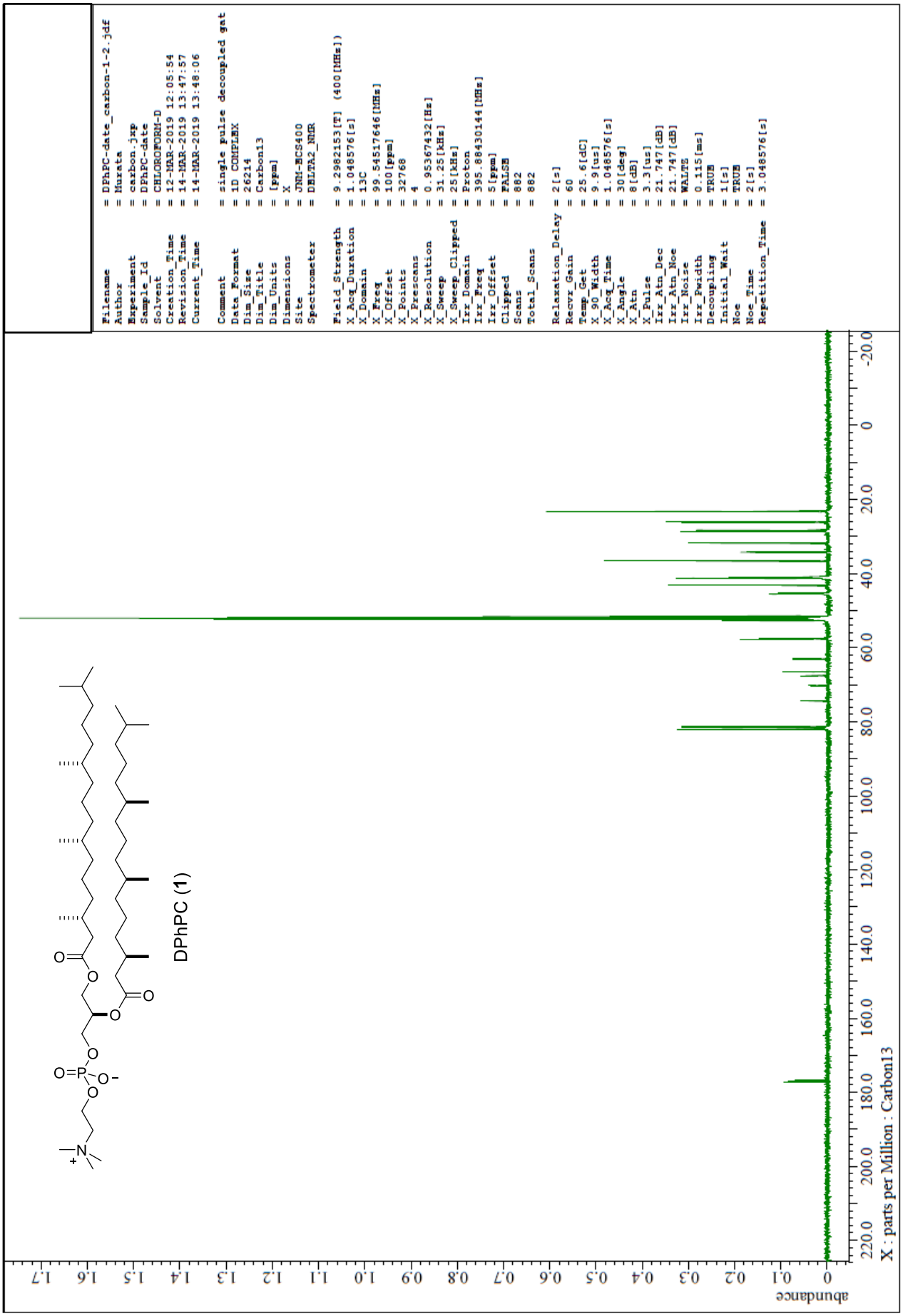
DPhPC (1)
abundance
X : parts per Million : Carbon13

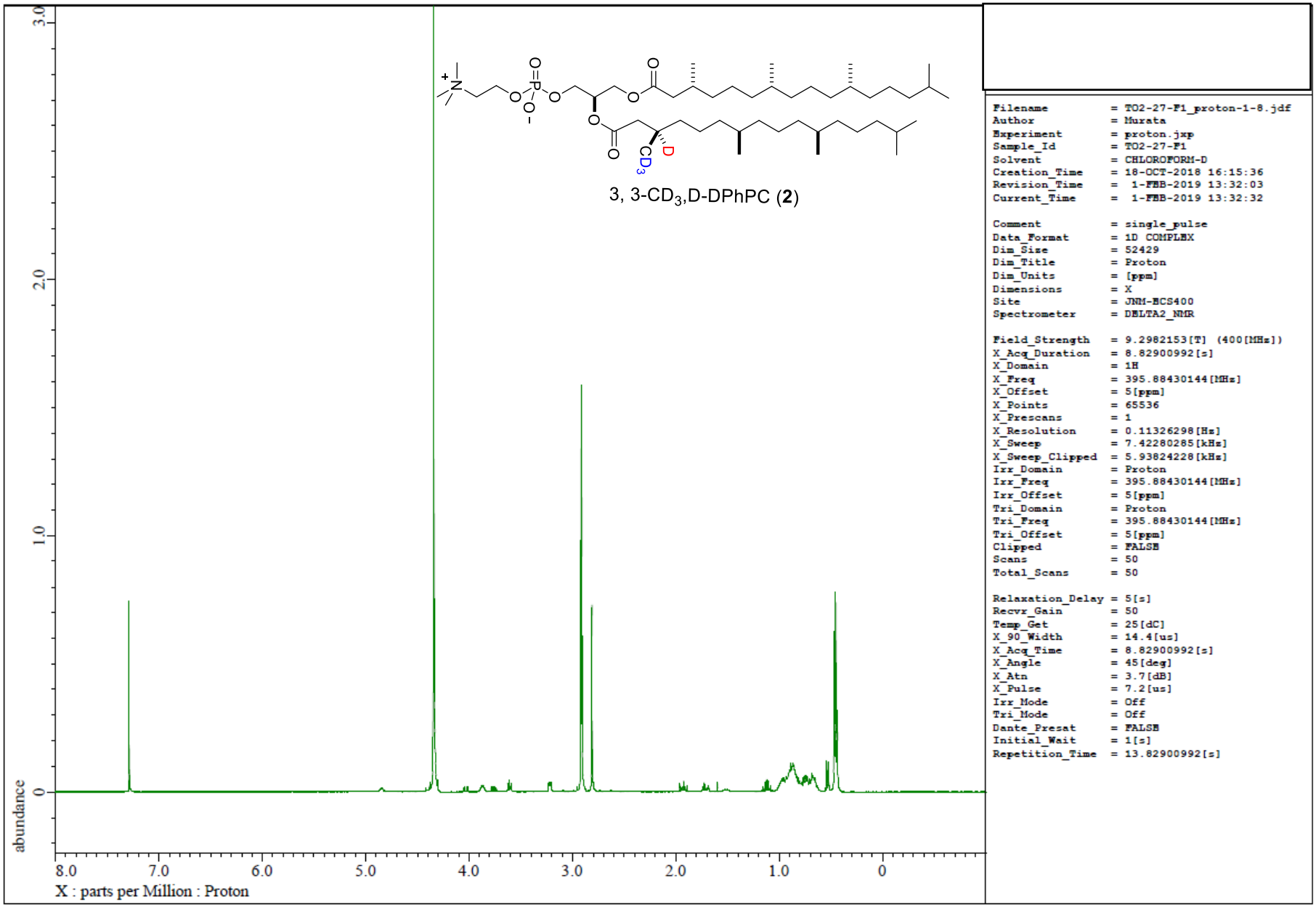

3, 3-CD_3,D-DPhPC (**2**)

```
Filename          = TO2-27-F1_proton-1-8.jdf
Author            = Murata
Experiment        = proton.jxp
Sample_Id         = TO2-27-F1
Solvent           = CHLOROFORM-D
Creation_Time     = 18-OCT-2018 16:15:36
Revision_Time     =  1-FEB-2019 13:32:03
Current_Time      =  1-FEB-2019 13:32:32

Comment           = single_pulse
Data_Format       = 1D COMPLEX
Dim_Size          = 52429
Dim_Title         = Proton
Dim_Units         = [ppm]
Dimensions        = X
Site              = JNM-ECS400
Spectrometer      = DELTA2_NMR

Field_Strength    = 9.2982153[T] (400[MHz])
X_Acq_Duration    = 8.82900992[s]
X_Domain          = 1H
X_Freq            = 395.88430144[MHz]
X_Offset          = 5[ppm]
X_Points          = 65536
X_Prescans        = 1
X_Resolution      = 0.11326298[Hz]
X_Sweep           = 7.42280285[kHz]
X_Sweep_Clipped   = 5.93824228[kHz]
Irr_Domain        = Proton
Irr_Freq          = 395.88430144[MHz]
Irr_Offset        = 5[ppm]
Tri_Domain        = Proton
Tri_Freq          = 395.88430144[MHz]
Tri_Offset        = 5[ppm]
Clipped           = FALSE
Scans             = 50
Total_Scans       = 50

Relaxation_Delay = 5[s]
Recvr_Gain        = 50
Temp_Get          = 25[dC]
X_90_Width        = 14.4[us]
X_Acq_Time        = 8.82900992[s]
X_Angle           = 45[deg]
X_Atn             = 3.7[dB]
X_Pulse           = 7.2[us]
Irr_Mode          = Off
Tri_Mode          = Off
Dante_Presat      = FALSE
Initial_Wait      = 1[s]
Repetition_Time   = 13.82900992[s]
```

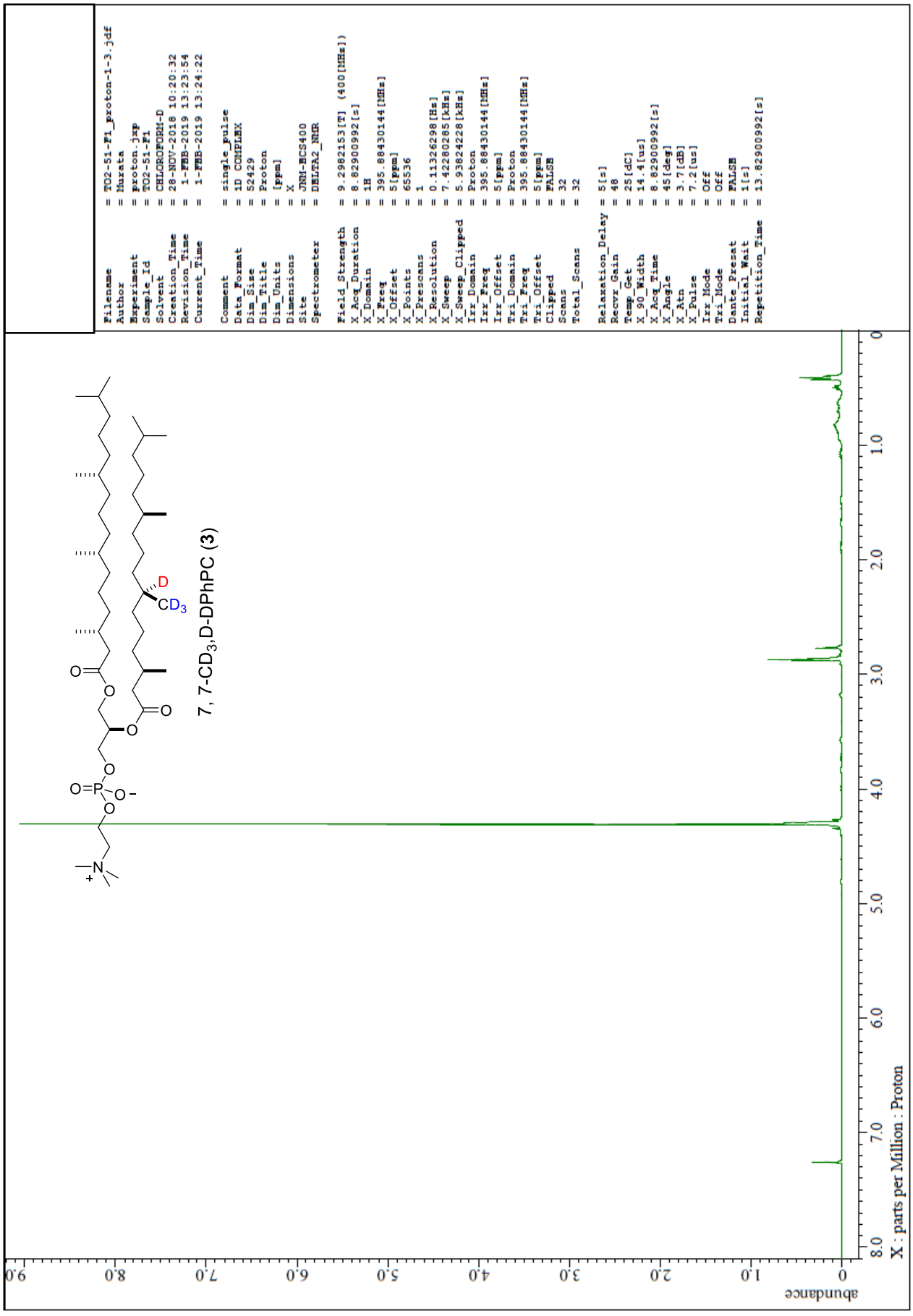
Filename = TO2-51-F1_proton-1-3.jdf
Author = Murata
Experiment = proton.jxp
Sample_Id = TO2-51-F1
Solvent = CHLOROFORM-D
Creation_Time = 28-NOV-2018 10:20:32
Revision_Time = 1-FEB-2019 13:23:54
Current_Time = 1-FEB-2019 13:24:22
Comment = single_pulse
Data_Format = 1D COMPLEX
Dim_Size = 52429
Dim_Title = Proton
Dim_Units = [ppm]
Dimensions = X
Site = JNM-ECS400
Spectrometer = DELTA2_NMR
Field_Strength = 9.29821153[T] (400[MHz])
X_Acq_Duration = 8.82900992[s]
X_Domain = 1H
X_Freq = 395.88430144[MHz]
X_Offset = 5[ppm]
X_Points = 65536
X_Prescans = 1
X_Resolution = 0.11326298[Hz]
X_Sweep = 7.42280285[kHz]
X_Sweep_Clipped = 5.93824228[kHz]
Irr_Domain = Proton
Irr_Freq = 395.88430144[MHz]
Irr_Offset = 5[ppm]
Tri_Domain = Proton
Tri_Freq = 395.88430144[MHz]
Tri_Offset = 5[ppm]
Clipped = FALSE
Scans = 32
Total_Scans = 32
Relaxation_Delay = 5[s]
Recvr_Gain = 48
Temp_Get = 25[dC]
X_90_Width = 14.4[us]
X_Acq_Time = 8.82900992[s]
X_Angle = 45[deg]
X_Atn = 3.7[dB]
X_Pulse = 7.2[us]
Irr_Mode = Off
Tri_Mode = Off
Dante_Presat = FALSE
Initial_Wait = 1[s]
Repetition_Time = 13.82900992[s]
7, 7-CD3,D-DPhPC (3)
D
CD3
O
O
O
O
O
O
O=P
O -
O
N
+
abundance
X : parts per Million : Proton
9.0
8.0
7.0
6.0
5.0
4.0
3.0
2.0
1.0
0
8.0
7.0
6.0
5.0
4.0
3.0
2.0
1.0
0